DRIVE-BY BRIDGE DAMAGE IDENTIFICATION THROUGH VIRTUAL SIMULATIONS

A Thesis
Submitted to the Graduate Faculty
of the
North Dakota State University
of Agriculture and Applied Science

By

Chang Liu

In Partial Fulfillment of the Requirements
for the Degree of
MASTER OF SCIENCE

Major Department:
Civil and Environmental Engineering

November 2019

Fargo, North Dakota

North Dakota State University
Graduate School

Title

DRIVE-BY BRIDGE DAMAGE IDENTIFICATION THROUGH VIRTUAL SIMULATIONS

By

Chang Liu

The Supervisory Committee certifies that this ***disquisition*** complies with North Dakota State University's regulations and meets the accepted standards for the degree of

MASTER OF SCIENCE

SUPERVISORY COMMITTEE:

Dr. Mijia Yang
Chair

Dr. Zhibin Lin

Dr. Ravi Yellavajjala

Dr. Jerry Gao

Approved:

01/16/2020
Date

Dr. David R. Steward
Department Chair

ABSTRACT

With massive infrastructures built in US, timely condition assessment of these infrastructures becomes critical to daily traffic and economics. Due to high cost, long time consumption of direct condition assessment methods, such as closing traffic for sensor installation and monitoring, indirect bridge monitoring has become a promising method. However, the technology is in its initial stage and needs substantial refinement. In this research, virtual simulation approaches, both in 2D and 3D, are used to model the bridge and vehicle interaction through ABAQUS. Artificial Damages were embedded to the model according to different locations and different levels of intensities. With the modelled outcomes, the hypothesis of identifying damages through the responses of the vehicle will be tested. From the simulated vehicle responses, bridge frequencies and damage locations and sizes could be identified accurately through short time flourier transformation and mode shape difference.

ACKNOWLEDGEMENTS

I would like to thank my advisor Dr. Mijia Yang, for his guidance and support, without whom this research would have been impossible.

I would also like to thank my respective graduate committee, Dr. Zhibin Lin, Dr. Ravi Yellavajjala, and Dr. Jerry Gao, for their invaluable input and guidance to complete this work.

I am thankful to my colleagues at my office, also my friends Xin Bai, Dawei Zhang, Xinyuan Yang, and Zi Zhang for their continuous support towards my completion of this thesis.

And finally, I want to thank the Department of Civil and Environmental Engineering at North Dakota State University for giving me the opportunity to complete this master's thesis.

DEDICATION

To my Parents, Qingfeng and Yuxia.

TABLE OF CONTENTS

LIST OF TABLES

LIST OF FIGURES

1. INTRODUCTION

1.1. Background and Literature Review

With massive infrastructures built in US, timely assessment of these infrastructure becomes critical to daily traffic and economics. Due to high costs and long-time consumption of direct condition assessment methods, such as closing traffic for sensor installation and monitoring, indirect bridge monitoring has become a promising method to manage the conditions of transportation infrastructure.

1.1.1. Indirect bridge monitoring

The idea of indirect bridge assessment that uses a passing vehicle to detect bridge dynamic properties was initiated by Yang et al. in 2004. They built a numerical model of a bridge vehicle system and studied the possibility of extracting bridge frequencies from the responses of vehicles (Yang, et al., 2004). This model assumes the displacement of a bridge can be described as a sinusoidal function,

$$u(x,t) = q_b(t)\, sin\left(\frac{\pi x}{L}\right) \tag{1}$$

The equations of motion for the sprung mass and the bridge can be written as

$$m_v \ddot{q}_v + k_v(q_v - u|_{x=vt}) = 0 \tag{2}$$

$$m\ddot{u} + EIu'''' = f_c(t)\delta(x - vt) \tag{3}$$

The contact force existing between the sprung mass and the beam can be expressed as

$$f_c(t) = k_v(q_v - u|_{x=vt}) + m_v g \tag{4}$$

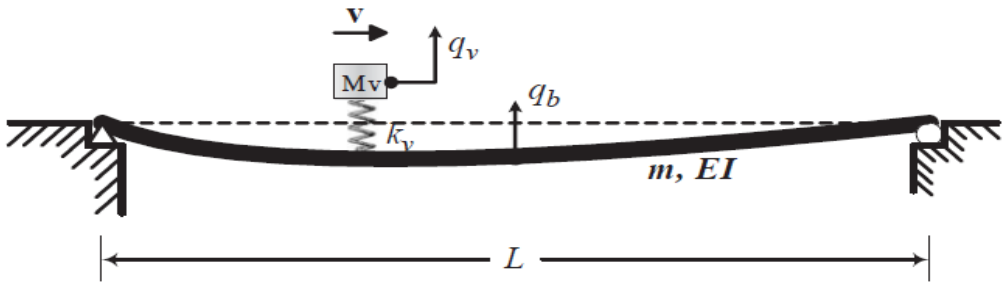

Figure 1.1. Sprung mass moving over a beam

Where $u(x, t)$ is the displacement of the bridge, x is the location of the vehicle on the bridge, L is the bridge span, $q_b(t)$ is the middle span deflection, m is the mass of the bridge, EI is the bending stiffness of the bridge, v is the vehicle speed, m_v is the vehicle mass, k_v is the contact stiffness between the vehicle and the bridge, q_v is the vehicle displacement, $f_c(t)$ is the interaction force between the bridge and the vehicle, and g is the gravity acceleration.

In their model, the vehicle vertical response is affected by the driving speed and the bridge to vehicle frequency ratio. Yang, et al. further proposed a finite element model and verified the accuracy of the concept (Yang, et al., 2009). The results clearly showed 4 frequencies in the acceleration spectrum, which are vehicle frequency, driving frequency, and two shifted bridge frequencies. However, the theoretical model is still a little far from being able to apply in practice, because the model does not consider vehicle damping and multi-lane effects of the bridge.

In another Yang and Lin's research (Yang and Lin, 2005), they studied more about the basic relationship of the vehicle-bridge system. In contrast to the previous model, the response of the bridge concentrates on its first vibration mode. The reason is that the vehicle, which acts as a moving force, cannot transfer much energy to trigger higher modes of a heavier bridge. Through comparison of the displacement, velocity and acceleration responses of the bridge under 5 different vehicle speeds, it was found that the acceleration response is more sensitive on extracting bridge frequencies. Another tested parameter is the damping of the vehicle. It was also found that the

damping will decrease the amplitude of the acceleration spectrum, which may cause difficulty in identifying bridge frequencies.

Yang, et al. further conducted a parametric study on this indirect method (Yang and Chang, 2009). In this work, a more complicated response function was derived to describe the bridge-vehicle system. In this function, the vehicle vertical response contains 4 frequencies: the vehicle frequency, the driving frequency, the left-shift bridge frequency, and the right-shift bridge frequency. The shifted bridge frequencies were also affected by the driving frequency. This study concluded that the initial vehicle/bridge acceleration amplitude ratio is important in identifying the bridge frequency. The smaller the ratio is, the greater the probability of successfully identifying the bridge frequencies.

Yang conducted a field test to verify the ability of an equipped vehicle in detecting bridge frequencies (Lin and Yang, 2005). In this test, a light truck with a trailer and a heavy truck were used. The data was collected from an equipped acceleration transducer inside the vehicle. 4 tests were performed under different conditions. In the first two tests, the heavy truck was acted as an excitation; while the responses of the bridge (test 1) and the deployed trailer (test 2) in the middle span were collected separately. The results showed that both responses can closely extract the bridge's first natural frequency. The amplitude of the acceleration spectra would increase as the truck speed increases. For the other two tests, the data was collected on a moving trailer towed by the light truck (test 3) and with the heavy truck moving simultaneously (test 4). Due to the trailer configuration and deck roughness, the authors showed that if the speed is higher than 40 km/h, it would be very difficult to identify the bridge frequencies.

Yang also had another study to build the mode shape from a passing vehicle (Yang, et al., 2014). In this study, the instantaneous amplitude history of the bridge component response can be

regarded as a mode shape. The bridge component response associated with special frequency can be extracted by using band-pass filters or singular spectrum analysis on the vehicle vibration response. Then the Hilbert transform is adopted to obtain the transform pair and the bridge instantaneous amplitude history. However, the amplitude history is always in absolute value, and the sign of the mode shape needs to be decided by engineers. A numerical study showed that lower vehicle speed guarantees higher accuracy of the mode shapes, and road surface roughness would make it difficult to extract the mode shape.

From Yang's study, it was verified that the bridge frequencies and mode shapes can be extracted from the responses of an equipped passing vehicle. And the parameter analysis was conducted on how accurate the method is under different conditions. Based on this theory, many other bridge properties were monitored through the vehicle responses by different investigators.

1.1.2. Further study on indirect bridge monitoring

González performed a multi-condition test of extracting bridge frequency using vehicles (González, et al., 2008). In this study, a 3D vehicle and bridge finite element models were built using MSc/NASTRAN software. In the simulation, the first natural frequency of the bridge is not found in various vehicle speeds. The second natural frequency can be extracted in low speed (under 20m/s). The problem is the accuracy of the extracted frequency is low. The experimental test also showed that some frequencies could be extracted from the equipped vehicle, but the bridge frequency would not show without enough excitation. The contributions of this study are that a 3D FEM model was established to simulate the BVI dynamic interaction and can be used to extract the frequency from the vertical acceleration responses of the vehicle. However, because the simulated vehicle has multi-degree of freedoms, the frequency spectrum showed many frequencies of the vehicle. Both simulation and practice test implied that adequate excitation is needed to

perform the bridge frequency extraction otherwise the bridge response would not show in the frequency spectrum due to negligible energy attributed to the fundamental bridge frequency.

González conducted a further study on extracting bridge frequency and damping (González, et al., 2010). The model adopted was a 2D half vehicle and bridge model simulated in MATLAB. 3 different length bridges with 5 different damping conditions were simulated. With increasing of the bridge length, the power spectrum (higher amplitude) will move to higher frequencies. If damping and the road roughness were taken into consideration, the acceleration spectra itself sometimes could not show the bridge frequency due to energy dissipation caused by damping and road roughness. However, the sensitivity of the PSD at all frequencies w.r.t changes of damping level can still show the bridge frequencies. The study confirmed that using vehicle to detect bridge frequencies with road roughness is very difficult. The damping sensitivities from PSD may show the bridge frequency. They conducted another damping identification research later (González, et al., 2012), the road roughness and vehicle initial condition were considered this time. The algorithm they developed has good accuracy in monitoring short span bridges (length under 15 m).

Zhang and his team performed a damage detection study based on the bridge mode shapes (Zhang, et al., 2012). They developed a model of which a vehicle with an excitation force moves on a 2D plate. In their theory, the amplitude of STFT acceleration spectrum is approximately proportional to the mode shape square (MOSS). And the mode shape square can show obvious differences between damage and undamaged parts. However, the MOSS can be extracted when the vehicle has much higher frequency than that of the bridge and the speed of vehicle cannot be faster than 2 m/s. In order to excite different mode shapes of the bridge, the vehicle needs to be equipped with a large force shaker. According to the test performed on two plywoods in dimension

of 150mm x 80mm x 5mm, the suggested MOSS method can exactly show the impact damage. In their study, STFT was used to extract more bridge information, but the limitations are the vehicle frequency and the low vehicle speed.

Li conducted a study on how to identify the damaged element using only extracted bridge frequencies (Li and Au, 2014). In this study, the fractional change of a frequency to the sum of multiple frequencies is equal to the damaged element fraction of model energy to the sum of that of multiple frequencies. This method could be used when the first several damaged and undamaged frequencies of bridge are extracted, and the mode shapes are simulated by finite element method. Comparison on the results of different frequencies will narrow down the range of possible damaged elements. It has been confirmed that if there was only one damage on an element, the damaged corresponding elements can be found. One limitation of this method is that enough data needs to be obtained to extract multiple frequencies. But how the length of element affects the identification needs to be tested in the future.

Sun used the curvature method to detect damages in his study (Sun, et al., 2016). The dynamic curvature will highlight the damage location. And this needs a displacement transducer to be installed at a position when a vehicle passes through the bridge. The numerical study showed that the dynamic curvature at the mid-point of a 15m bridge can indicate the approximate damage location. And the curvature is also sensitive to the damage intensity. However, this method still needs the sensor deployment on bridge, while the vehicle just acts as a moving force.

O'Brien and Malekjafarian conducted a study on how to extract mode shapes using multiple vehicles (O'Brien and Malekjafarian, 2014). They simulated the BVI model as a 2D beam with 2 quarter-vehicles. To obtain the mode shapes, Singular Value Decomposition (SVD) was applied to the power spectral density matrix. The bridge was divided into several parts, and each

part has the same length as the distance of the 2 quarter-vehicles. These two vehicles started at the two ends of the first part and moved at the same speed. After fully moving through a segment, fourier transformation is applied to the vertical acceleration of each axle. SVD is then applied to each spectral density. In a case study for a bridge of 15 m, the SVD method can correctly extract the first two mode shapes. It was also confirmed that bridge mode shapes could be found through a truck and two trailers. This method can extract mode easily from the acceleration history of two moving vehicles. However, the results are 2 points' modes of each segment, which may be not fine enough to identify damage on a bridge.

O'Brien and Malekjafarian also used this method to detect damage (O'Brien and Malekjafarian, 2016). In this study, they mentioned that the resolution of original Short Time Frequency Domain Decomposition (STFDD) may not be adequate. However, the segment size cannot be too small otherwise shorter signals may give inaccurate results. In order to improve this method, several laser vibrometers are added on the two-axle vehicle. The vibrometer can detect the relative velocity between vehicle and road, through which vehicle body acceleration history and the bridge velocity at the contact point can be extracted. And the segment number can be increased by decreasing time spacing between signals with multi laser vibrometers. According to the case study, the damage location can be identified from the extracted MOSS compared with the undamaged MOSS. And the speed of test vehicle can be increased to 8m/s. If there is noise, small damages still can be detected. This continuous study improved the STFFD method and tested the ability of damage location identifications, where the damage indicator is based on the largest difference between damaged and healthy MOSS. This may not work with multiple cracks.

Kong and his team also adopted the multiple axle BVI model to extract frequency and modal property (Kong, et al., 2016). They used the residual response of moving vehicles to extract

bridge properties. The residual response is the vertical displacement difference of two moving vehicles. The vehicles pass the bridge with a time difference. And the residual response is calculated from the difference of 2 vehicle's vertical displacements at the same location. It is found that it is more efficient to use the residual response rather the single axle response in identifying mode properties. More bridge frequencies and the mode shape squares can be extracted from the residual responses, which are very close to the true value in the first two modes. In Kong's another research (Kong, et al., 2017), he used the two vehicle models to test the residual response method. One model still uses the single -degree-of-freedom vehicles, while another model uses a five-axle truck model. And the results show that the multi-DOF model has better performance for extracting mode shapes. The residual response mothed shows another possible way of monitoring bridge properties.

Nguyen and Tran adopted another analysis method to detect damages (Nguyen and Tran, 2010). They used a 2D 2-axle vehicle and a beam bridge model to build the BVI model. And the cracks of the bridge were represented by the changes in stiffness. After the vehicle moved through the bridge, the displacement history was obtained and investigated. When the vehicle speed remains at 2 m/s, the peaks of the wavelet analysis results become more significant with increase of crack depth. And the identification of small damages can be revealed with low speed vehicles, while the high-speed vehicle can only identify cracks with deeper than 50% of the beam height. The case study also includes the effect of noise. If the noise level does not exceed 6%, the wavelet method could be used to detect damage.

Hester and González also used the wavelet method to detect damage in beam-like structures (Hester and González, 2012). They collected the bridge vertical acceleration data when a vehicle passed the bridge. If the wavelet transform is conducted on the collected data, the results will show

the damage if its size is large enough, and the wavelet coefficient .vs. position plot can indicate the damage location. If more sensors and multiple scales are used, the wavelet method will give significantly better results than the single sensor and the single scale do. In the test of a simulated beam with crossing of a sprung vehicle model, it showed that the data collected from bridge needs to be trimmed to remove the bridge edge effect. Overall, the accuracy of wavelet method is not perfect, but it shows the possibility of identifying damage location on a bridge. However, this method still uses the vehicle as moving loads, and sensors need to be deployed on the bridge.

McGetrick and Kim developed another wavelet-based monitoring method (McGetrick and Kim, 2013). They used the data collected from a passing vehicle and analyzed the behavior of the bridge. The study adopted a BVI model with a 2-axle vehicle. Each axle has an accelerometer. The Morlet continuous wavelet transform will be applied to the acceleration data to get the wavelet coefficients. And the damage index would be calculated through comparing the CWTs of accelerations obtained in theoretical simulations and experiments. The peaks in the differences between the damaged and undamaged results showed the locations of damages. Parameter study found that bridge length, damage level, and vehicle speed have positive correlations with the wavelet peak value. With the vehicle speed increasing, the bridge and vehicle interaction time is shortened, which could cause a decreasing resolution.

As for modelling of bridge and vehicle interactions, there are many excellent works in literature. Oliva and his team built a detailed 3D BVI model using Abaqus (Oliva, et al., 2013). In this study, the vehicle model is simulated as a 3-part model with 7-DOF. The first seven natural frequencies and relative mode shapes are extracted in Abaqus. The vertical displacements of vehicle and mid-bridge are simulated with different class road profiles. Based on this work, a 3D Abaqus BVI model was established and adopted in this thesis.

1.2. Research Objectives

This study focuses on drive-by inspection of bridges through numerical simulations. Previous study has shown multiple methods to detect bridge properties. However, identifying damages through drive-by vehicle responses is the main aim of this study.

The primary objectives of this study are,

- To build 2D and 3D Bridge-Vehicle-Interaction models in Abaqus, and to validate the finite element model through literature results.
- To simulate different bridge damage conditions, find the connection between responses of drive-by vehicles with damage details.
- To perform a parametric study and evaluate damages through the FFT, STFT and mode shape difference method.
- To simulate road roughness in a 3D bridge-vehicle-interaction model, and to study its effect on damage detection of the suggested drive-by method.

1.3. Organization of the Thesis

This thesis consists of five chapters and the following summarizes the content of each chapter,

- Chapter 1: Introduction and literature review which include background to the drive-by bridge inspection, the bridge vehicle interaction modeling, the objectives and organization of the thesis.
- Chapter 2: 2D bridge-vehicle-interaction model generation and verification, parametric study using the FFT, STFT and mode shape method for damage detection.
- Chapter 3: 3D bridge-vehicle-interaction model generation and verification, parametric study using the FFT, STFT and mode shape method for damage detection.

- Chapter 4: Simulation of road roughness and effect of road roughness on drive-by bridge inspection.
- Chapter 5: Conclusion and recommendations for future work.

2. DRIVE-BY DAMAGE IDENTIFICATION THROUGH 2D VIRTUAL SIMULATIONS

2.1. Introduction

As discussed in Chapter 1, drive-by inspection is an excellent candidate to efficiently inspect vast bridges. However, the technology is in the initial stage and needs substantial refinement. In this chapter, a 2D virtual simulation approach is used to model the bridge and vehicle interaction. With the modelled outcome, the hypothesis of identifying damages through the responses of the vehicle will be tested under different bridge, vehicle, and damage parameters.

In this chapter, the numerical model is first created in ABAQUS, which is then validated through the literature results. Damages on the bridge are then simulated through reducing the element stiffness at different locations and different extensions. The outcome responses of the vehicles are further processed and used to extract the damage location and intensity.

2.2. Model Creation

In this part, a 2D BVI model is built in ABAQUS to simulate the dynamic responses of bridge and vehicle interaction. The example used by Liu and his team (Liu, et al.,2008) is adopted, in which the 2D BVI model has three parts: a sprung mass acts as the vehicle, a simply supported beam acts as the bridge, and a rigid point acts as the tire.

The bridge part is simulated as a 2D beam. In order to make the moment of inertia equal to 2.9 m^4, the profile of the cross section is selected as a 4.35 m x 2 m rectangle. The given density of the material is 2303 kg/m, and the linear density of the member can be calculated from the cross area, which is 264.71 kg/m^3. Young's module of the material is 2.87e9 Pa, and its Poison's ratio is 0.3. The length of bridge is 25 m. The element type is chosen as beam and its meshing size is set as 0.05 m to grantee the modeling accuracy.

In order to verify the numerical convergence, the displacements of bridge mid-span under vehicle load are compared when the mesh size are 1 m, 0.5 m, 0.25 m, 0.1 m,0.05 m and 0.02 m. From Figure 2.1, when mesh size is below 0.25 m, the displacement converges to 0.00223 m with negligible differences.

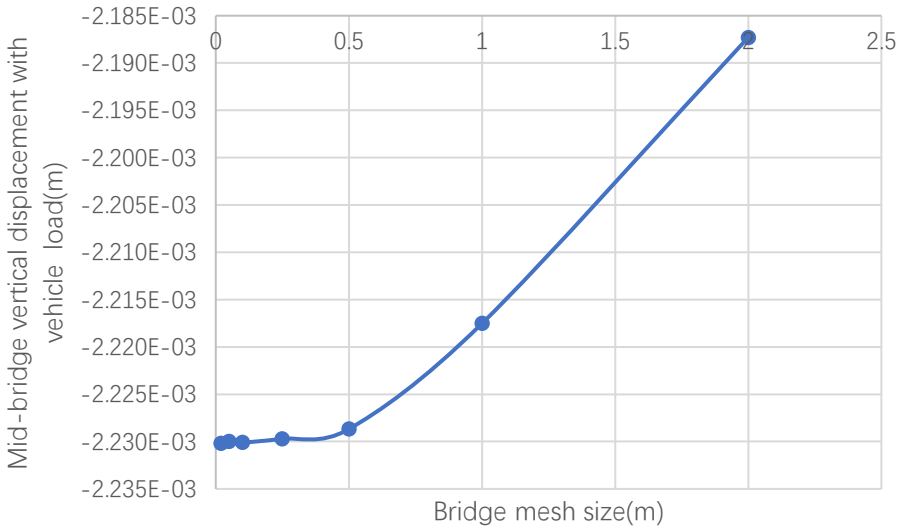

Figure 2.1.Convergence of mid-span displacement with respect to the mesh size used

The vehicle is also modeled as the beam element in this chapter. The profile of the vehicle is a 1 m x 1 m rectangle. The length of the beam is 1 m, too. The density of the material is 5707 kg/m^3, which leads to the mass of the vehicle equal to 5707 kg. The Young's module is 2.87e11 Pa. Since the vehicle is modelled as a mass-sprung system, the beam is kept short in order to avoid the vibration modes of the beam mass itself.

The tire of the vehicle model is simulated as a point mass, which is a rigid body with an assigned mass of 1 kg (Figure 2.2).

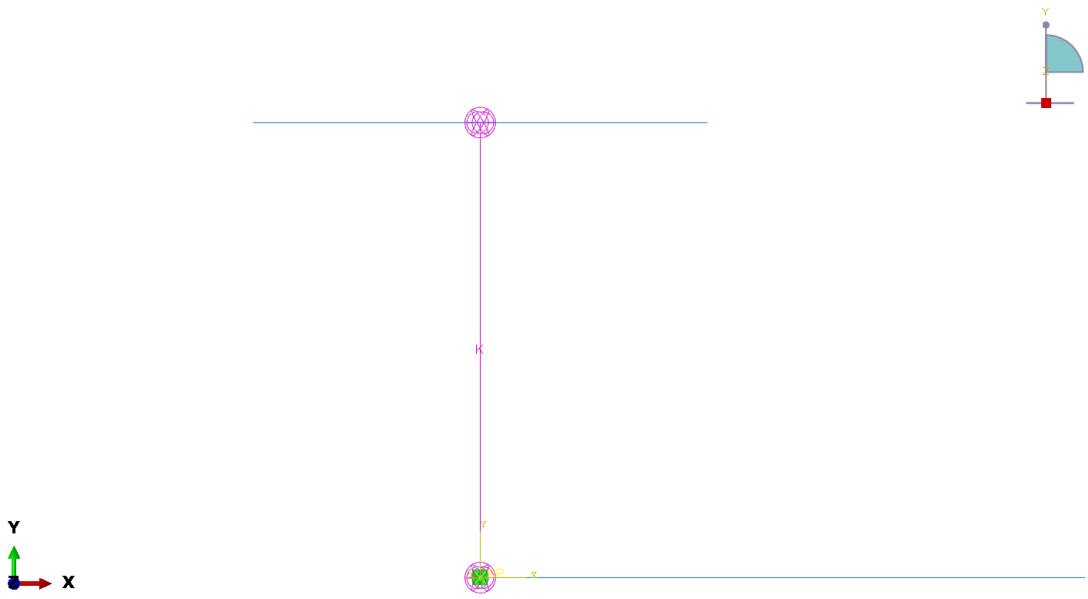

Figure 2.2. Spring connection between the vehicle body and the tire point

To assembly the model, the vehicle mass part is set 1 m above the left end of the bridge. The tire point has the same coordinate as that of the left end point of the bridge. A spring which has a stiffness of k=0.5e7 N/m is connected between the mid-point of the vehicle mass and the tire. To correctly model the bridge-vehicle interaction, the bridge part and the tire have a hard and surface-to-point contact. The boundary conditions of the bridge are set like this: the left end is pinned support and the right end is roller supported, with a restraint on the vertical displacement. All these settings are set in the initial step of the ABAQUS model.

In the second step, a gravity load is added onto the vehicle mass part. A static analysis is conducted thereafter, which simulates the vehicle gravity load on the model (Figure 2.3).

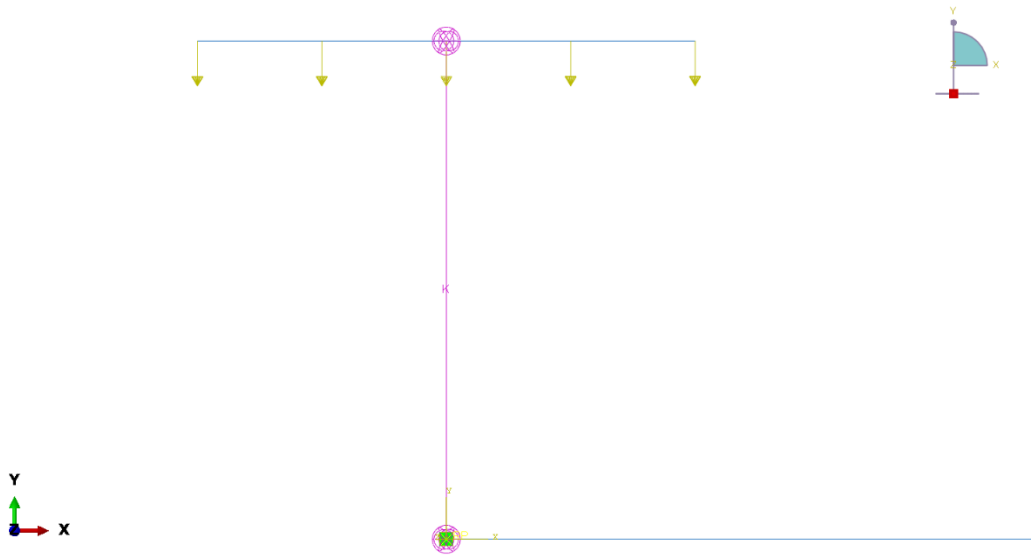

Figure 2.3. Apply gravity load of the vehicle

In the third step, the vehicle mass and tire parts are applied with a 27.7m/s horizontal velocity (Figure 2.4). The whole step lasts 0.9 s, and a dynamic, implicit analysis is performed to simulate the bridge-vehicle interaction along the whole bridge.

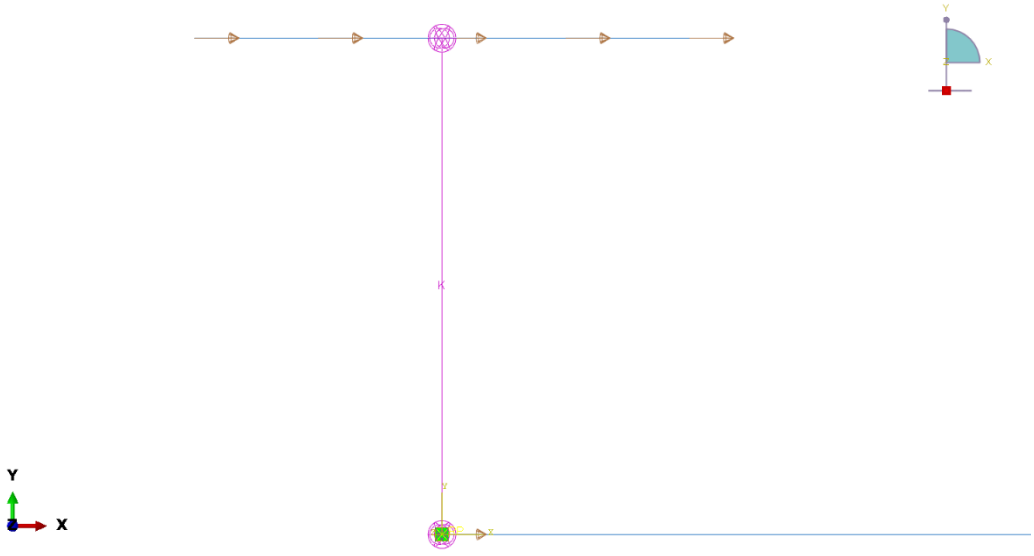

Figure 2.4. Apply vehicle speed

After completion of the analysis, the mid-point vertical displacement of the bridge is extracted and compared with the literature results of the reference. And the comparison plot is shown in Figure 2.5.

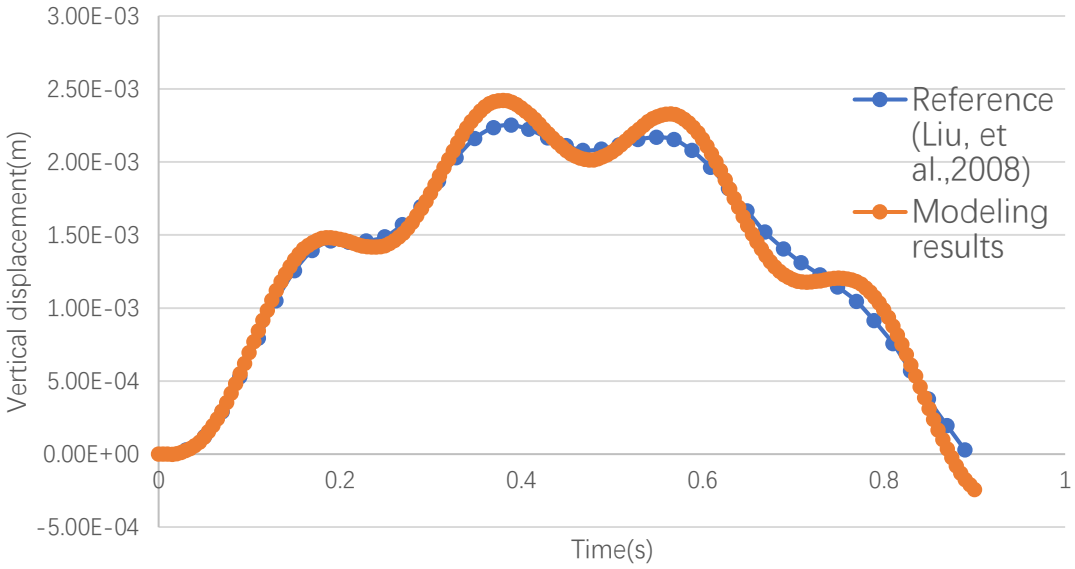

Figure 2.5. Comparison of mid-point displacements between the literature and the Abaqus modeling results

From Figure 2.5, one can see the ABAQUS modeling results are almost the same as the displacement result of reference, with a maximum difference of 5.1%.

2.3. Effect of Damage on Bridge Frequencies

In order to compare effects of different damages to the bridge, 12 damage models are created in this part as shown in Table 2.1.

Table 2.1.List of damaged model conditions

Model	Location	Elasticity	Size
1			0.1m
2	1m	20% loss	0.5m
3			1m
4			0.1m
5	5m	20% loss	0.5m
6			1m
7			0.1m
8	10m	20% loss	0.5m
9			1m
10		20% loss	
11	12.5m	40% loss	0.1m
12		60% loss	

Two damage factors are simulated in the model: one damage factor is the damage location; while the other factor is the damage intensity. Three different damage locations and three damage intensities are simulated in this model.

A healthy bridge of the example (Liu, et al., 2008) is simulated first. From the results obtained in Section 2.2, the frequency of the bridge can be more easily extracted from the responses of a low speed vehicle. Based on this reasoning, the speed of Abaqus moving vehicle is decreased to 1 m/s, and it takes 25 s for the vehicle to pass through the bridge. The time step used in the dynamic step is 0.001 s in order to grantee the model stability. The time history of the vertical acceleration of the vehicle is recorded and shown in Figure 2.6. 3 frequencies are successfully extracted from the Fast Fourier Transform (FFT) analysis of the vertical acceleration of the vehicle (Figure 2.7).

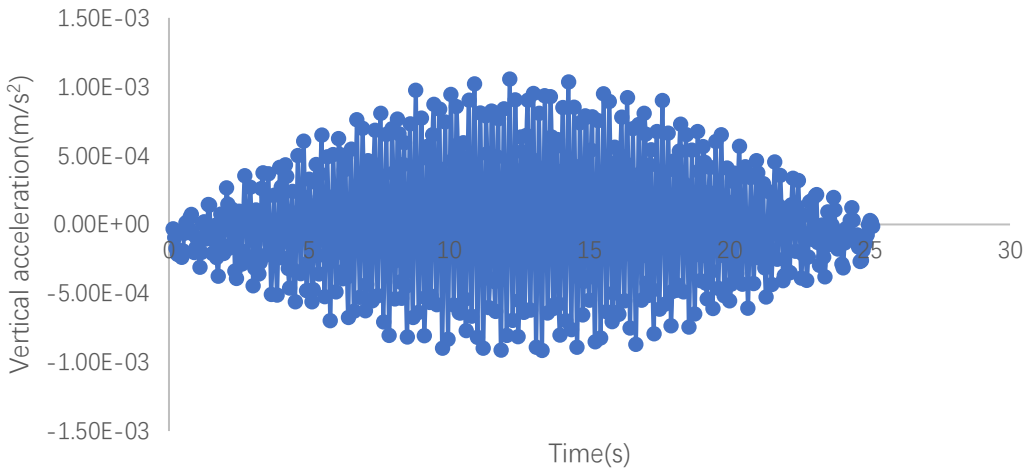

Figure 2.6. Vertical acceleration history of the vehicle

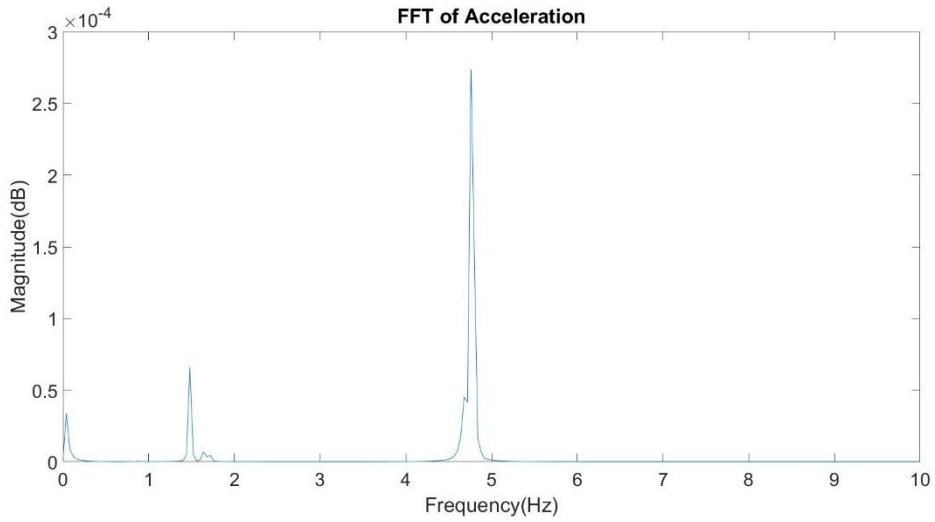

Figure 2.7. Fast Fourier transform results of the vehicle vertical acceleration history on the original bridge

In the frequency spectrum plot (Figure 2.7), the bridge frequency is about 4.76 HZ, the vehicle frequency is about 1.48 HZ, and the driving frequency is about 0.04 HZ. The three frequencies match well with the results in the reference.

Based on the validated healthy bridge model, the above mentioned damage cases are embedded in the model and simulated. 3 model cases are created to study the effect of different damage locations, which are at the location of 1 m, 5 m and 10 m from the left end of the bridge. The damage is simulated as a 1 m long segment in the bridge with half the Young's modules of other elements. Other properties are kept the same as before. The simulated vertical acceleration data of the vehicle are recorded and used to extract the frequencies. The first frequency of the bridge with damage at 10 m, 5 m and 1 m location is 4.6 HZ, 4.68 HZ, and 4.76 HZ respectively (Figure 2.8). The results show that the decrease of bridge frequency has a linear relationship with respect to the distance between the support and the damage location. For damages close to the support, the resulted frequency does not change compared to that of the healthy bridge. This is

reasonable since the damage close to support does not largely affect the bridge global stiffness, compared to the damages in the center of the bridge.

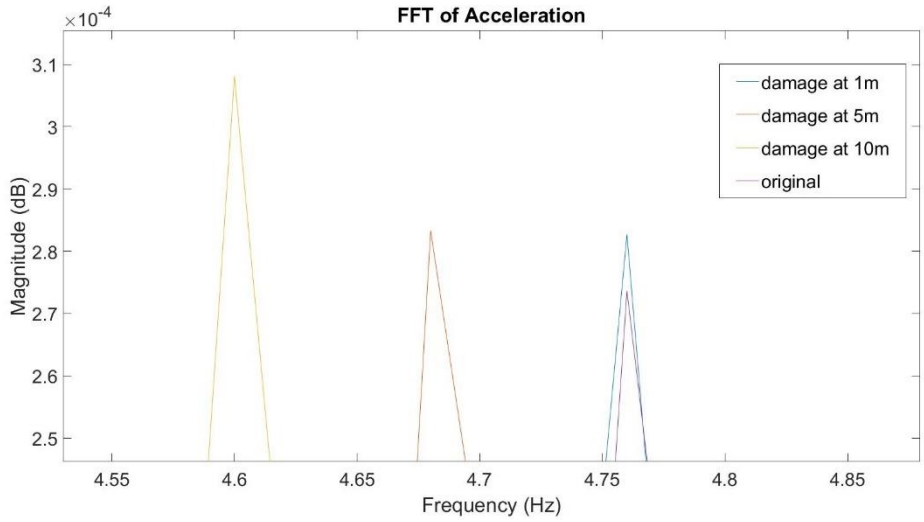

Figure 2.8. Fast Fourier transform results of the vehicle vertical acceleration history on the bridge with different damage locations

A symmetric damage pattern is also simulated. The results show that if the damage location is symmetrical about the mid span of the bridge. The identified frequency would be the same (Figure 2.9).

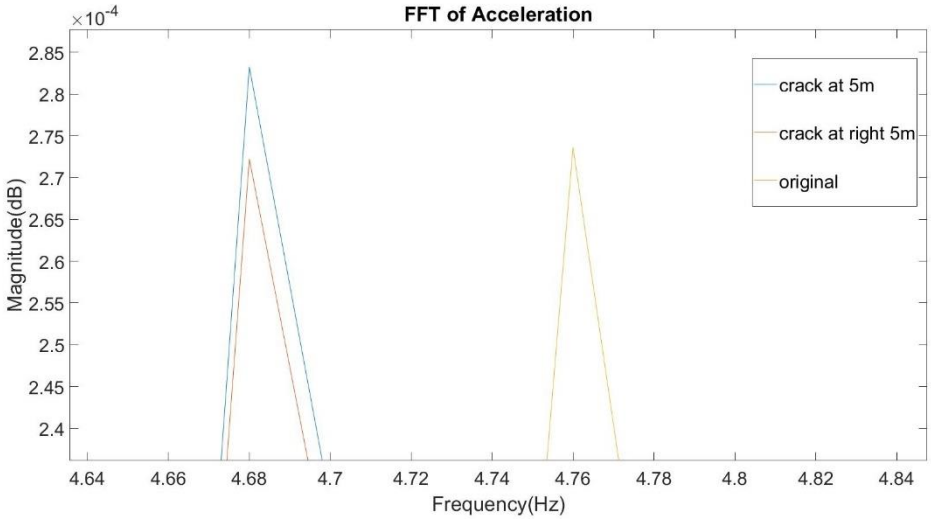

Figure 2.9. Fast Fourier transform results of the vehicle vertical acceleration history on the bridge with symmetrical damage

Another 3 model cases are created to study the effect of different damage levels. The Young's modulus of an 1 m long segment of the bridge at the 10 m location from the left support is reduced by 20%, 40% and 60% compared to its original Young's modules. The identified first frequency of the bridge is 4.72 Hz, 4.64 Hz, and 4.52 Hz respectively (Figure 2.10).

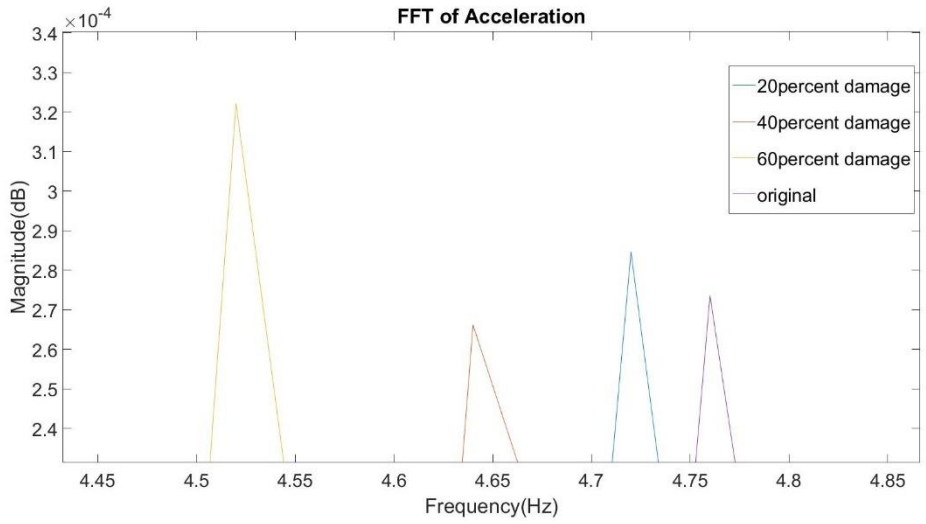

Figure 2.10. Fast Fourier transform results of the vehicle vertical acceleration history on the bridge with different damage levels

In order to study the sensitivity of the vehicle responses to damage sizes, 4 damage sizes at each damage location are simulated. The damage is still being simulated as only having half the Young's modules as these of other elements. The damage sizes are chosen as 1 m, 50 cm, and 10 cm respectively.

At the 1 m damage location, the sensitivity of the damage size is very low. It is apparently that only the amplitude of the frequency spectrum changes, but not the frequency value (Figure 2.11).

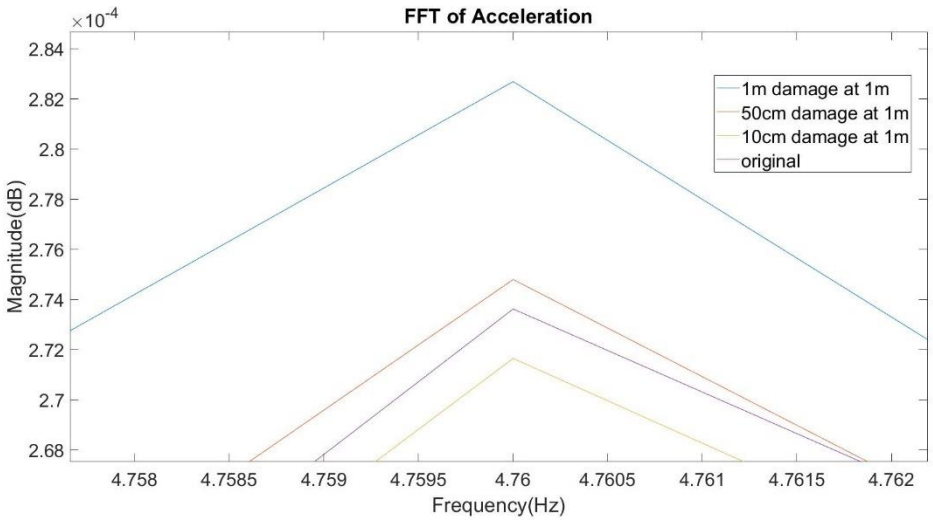

Figure 2.11. Fast Fourier transform results of the vehicle vertical acceleration history on the bridge with different damage sizes at 1m

At the 5 m damage location, the identified bridge frequency for the damaged bridge with an 1 m, 50 cm, and 10 cm length damage is 4.68 Hz, 4.72 Hz, and 4.76 Hz, respectively. It could be found that the identified bridge frequency reduces as the length of the damage segment increases (Figure 2.12).

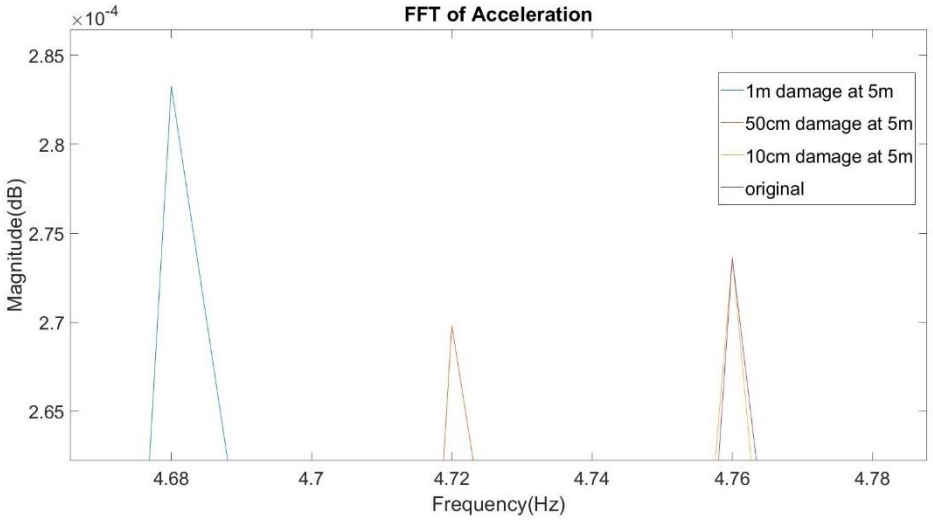

Figure 2.12. Fast Fourier transform results of the vehicle vertical acceleration history on the bridge with different damage sizes at 5m

At the 10 m damage location, the identified frequency of the bridge with the 1 m, 50 cm, and 10 cm length damage is 4.6 Hz, 4.68 Hz, and 4.86 Hz, respectively (Figure 2.13). Similar trend is found as the case with a damage at the 5 m location.

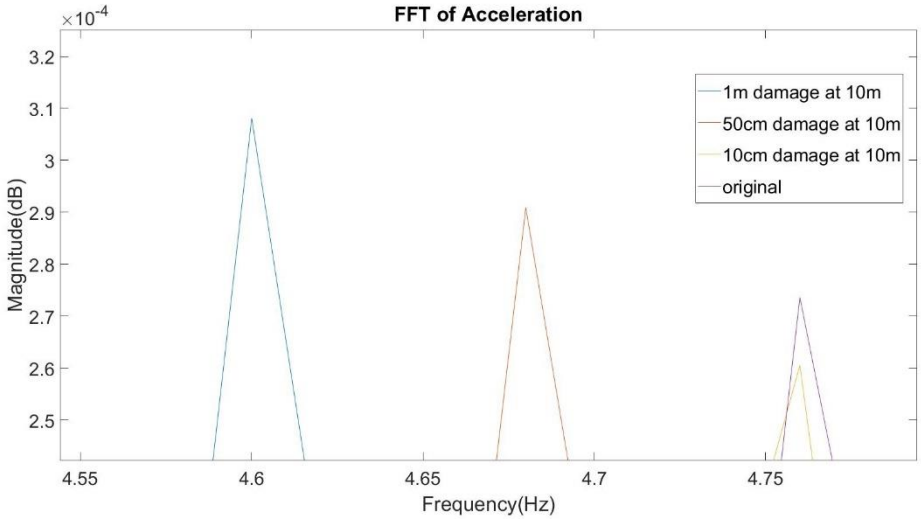

Figure 2.13. Fast Fourier transform results of the vehicle vertical acceleration history on the bridge with different damage sizes at 10m

2.4. Short Time Fourier Transform Results

Short Time Fourier Transform (STFT) analysis is an advanced signal processing tool and provides another dimension on the frequency change with time, which will be very helpful to process the vertical acceleration data and locate the damages.

The effect of different window's size is researched first. 5 different window sizes are selected, which are 10, 20, 50, 100, and 250 respectively. The vertical acceleration data from the vehicle on the health bridge is studied first (Figures 2.14-2.18).

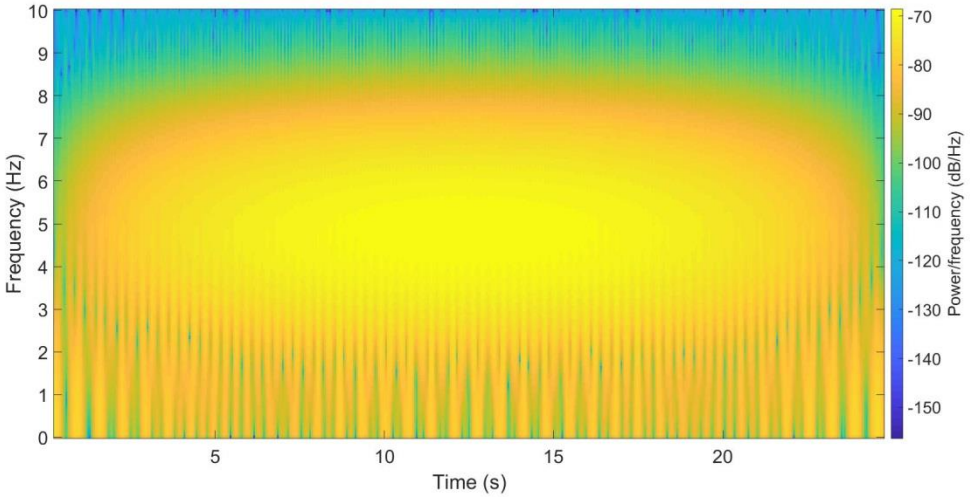

Figure 2.14. Short time Fourier transform results of the vehicle vertical acceleration history on the original bridge with window size 10

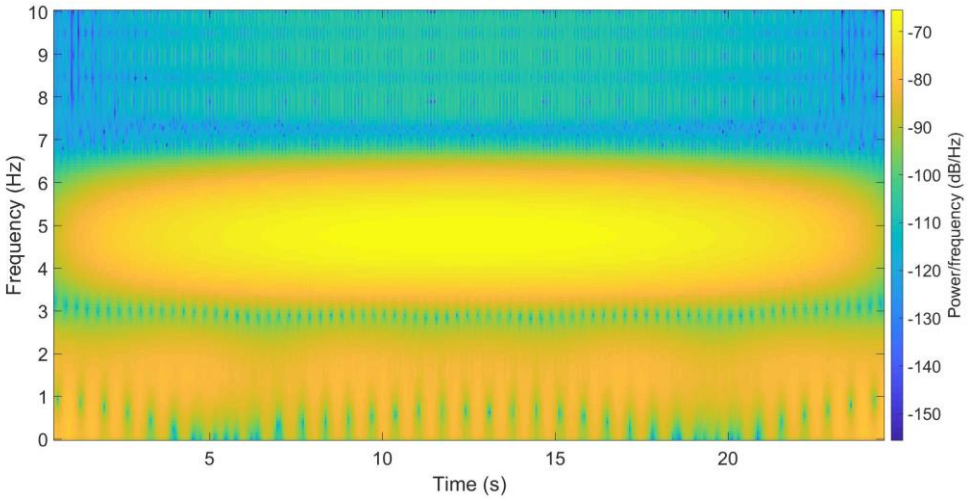

Figure 2.15. Short time Fourier transform results of the vehicle vertical acceleration history on the original bridge with window size 20

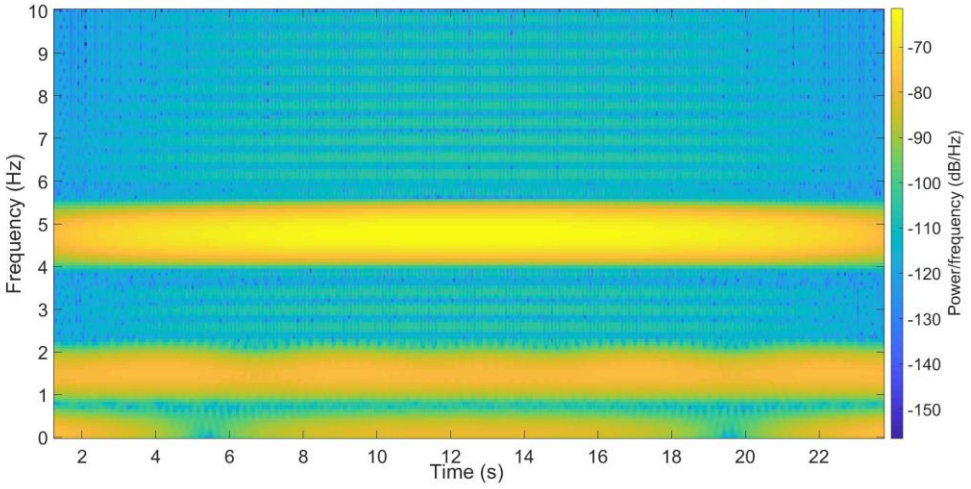

Figure 2.16. Short time Fourier transform results of the vehicle vertical acceleration history on the original bridge with window size 50

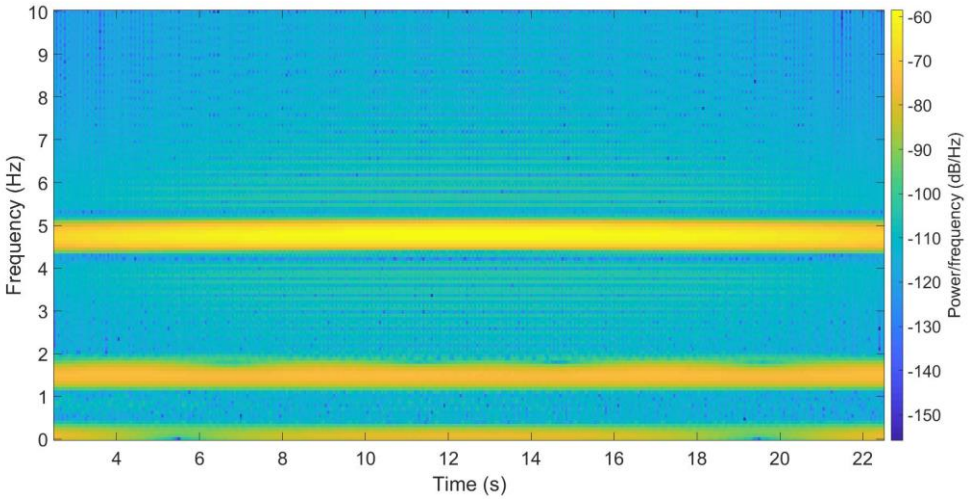

Figure 2.17. Short time Fourier transform results of the vehicle vertical acceleration history on the original bridge with window size 100

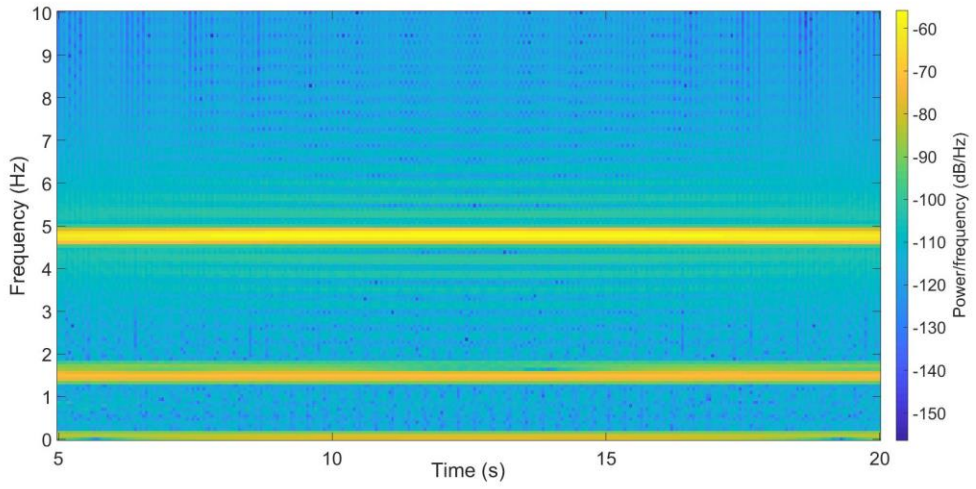

Figure 2.18. Short time Fourier transform results of the vehicle vertical acceleration history on the original bridge with window size 200

From the results of Figures 2.14-2.18, we can see that the STFT results with larger window will get better resolution. However, this function has a disadvantage. The results of STFT will lost some data at the beginning and ending of the signal. And the number of lost data is equal to half number of the window length. In another words, more data will be lost with larger window. In this way, the window needs to be controlled in a suitable range. As for this research, the rest study will use 100 window length.

When the damage exists, the STFT results will show that the color of some area is changed, which means the frequency energy of indicated areas are changed. Figure 2.19 presents the results of the 1m-length-damage-at-5m bridge.

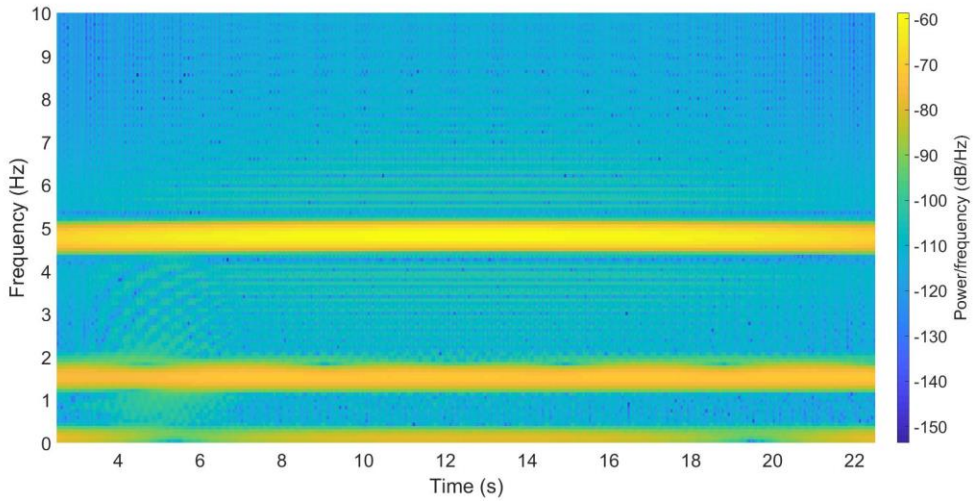

Figure 2.19. Short time Fourier transform results of the vehicle vertical acceleration history on the bridge with damage at 5 m location

All damaged cases show the same changing pattern, which is the energy of the low frequency range will increase at different locations. In this way, the energy of frequency ranging from 0.39 Hz to 1.10 Hz is analyzed to find the relationship between the STFT results and different damage cases.

In order to identify the damage location, a basic energy line is set from the healthy bridge results (Figure 2.17). The average energy of aimed range frequency is -113.08 dB, and it could be assumed that if 5% change to the energy happens, the location could be marked as a damaged area. As for this study, the identified damaged area starts when the average energy becomes constantly larger than -107.7dB.

For different damage locations, the mid locations of damage areas are compared between real cases and identified results and shown in Table 2.2.

Table 2.2. Comparison of STFT results of different damage locations on the bridge

Cases	Real mid location(m)	Identified results			
		Start location (m)	End location (m)	Mid location (m)	Ave energy (dB)
1 m damage at 1 m location	1.5	2.5	3.45	2.975	-101.06
1 m damage at 5 m location	5.5	3.25	7.85	5.55	-97.234
1 m damage at 10 m location	10.5	8.05	12.95	10.5	-95.321

From Table 2.2, the damage locations identified are close to the real cases at 5 m and 10 m locations. For the 1 m damage location case, 50 data (2.5 m long) are lost due to the STFT analysis, which leads to the not-so-accurate damage identification at this case.

For different damage sizes, the mid locations of damage areas and damaged lengths are compared between the real sizes and the identified results.

Table 2.3. Comparison of STFT results of bridges with different damage sizes

Cases	Real mid location (m)	Real damaged length (m)	Identified results				
			Start location (m)	End location (m)	Mid location (m)	Damaged length (m)	Ave energy (dB)
1 m damage at 10 m location	10.5	1	8.05	12.95	10.5	4.9	-95.321
0.5 m damage at 5 m location	10.25	0.5	8.05	12.4	10.225	4.35	-93.278
0.1 m damage at 10 m location	10.05	0.1	8.5	11.6	10.05	3.1	-101.667

Table 2.3 shows that for different size damages, damage location identification still works fine. However, the identified damage sizes are not consistent with the real sizes. This may be caused by the chosen basic energy line.

For different damage levels, only the energy zone at the damaged area is analyzed. The damaged area is at the 10 m to 11 m location of the bridge. The energy change with respect to different damage levels is summarized and shown in Figure 2.20.

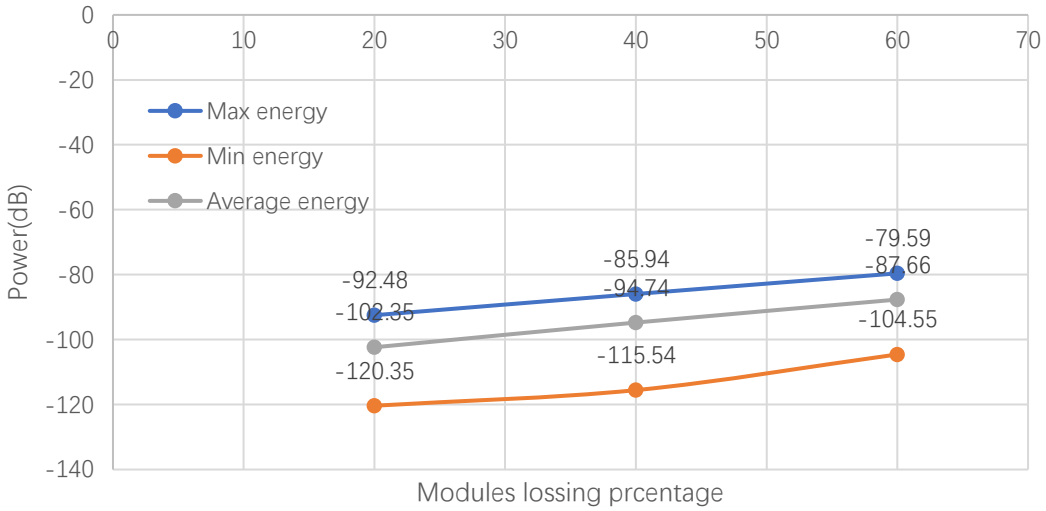

Figure 2.20. Comparison of STFT results of the vehicle vertical acceleration history on the bridges with different damage levels

Figure 2.20 shows that the energy loss of the damage area has a linear relationship with the damage level, which could be used to identify the damage level once the STFT spectrum of the vehicle vertical acceleration is generated.

For multiple damages, 1 m damages are set at the 5 m, 10 m and 20 m locations, the results of the STFT on the vehicle vertical acceleration is shown in Fig 2.21

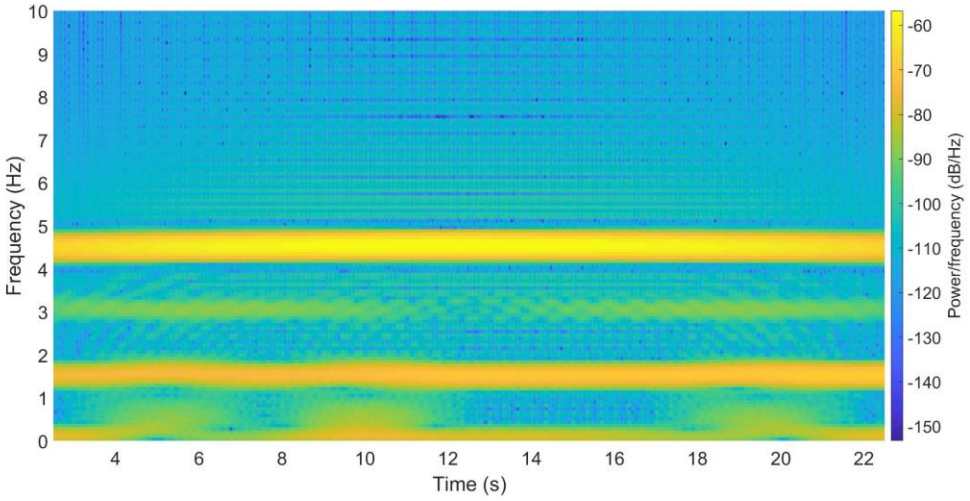

Figure 2.21. Comparison of STFT results of the vehicle vertical acceleration history on the bridges with multiple damages

Figure 2.21 showed that for multiple damages the STFT method can still work. Changes of frequencies and energy leaked at the damage zones can be identified according to the damage locations.

2.5. Mode Shape Analysis Results

The results on vehicle vertical accelerations of the ABAQUS simulations are also analyzed by the mode shape method. The method is based on Yang's mode shape construction theory. Using a filter function, the bridge response history can be extracted from the vehicle displacement history through Matlab. Then the Hilbert-Huang transform can be used to obtain the mode vector of the bridge response history and form the mode shapes of the bridge at particular frequencies (Figure 2.22).

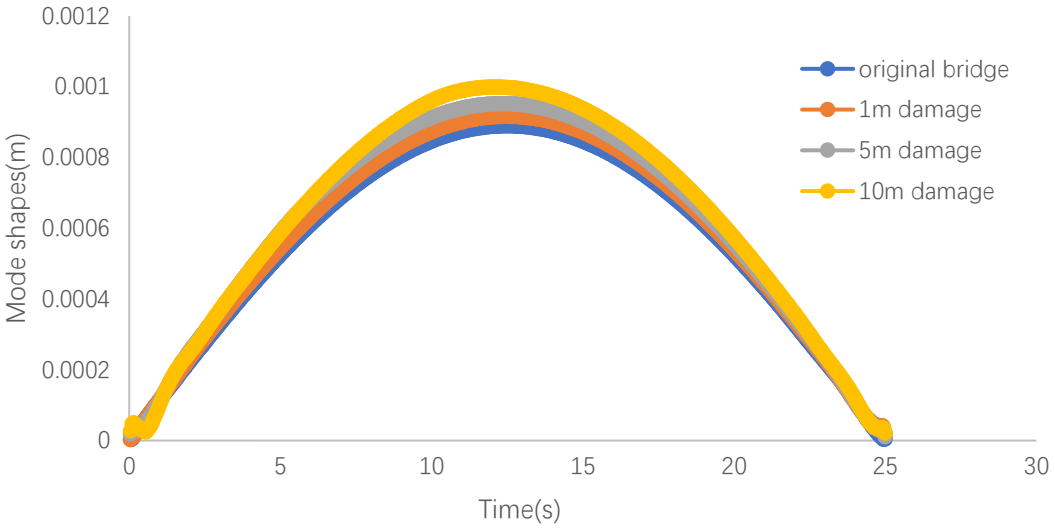

Figure 2.22. Mode shape extracted using Hilbert transform

The differences between the original bridge and the damaged bridge mode shapes will show the locations of damaged sections. The results are shown in Figure 2.23. 2-25.

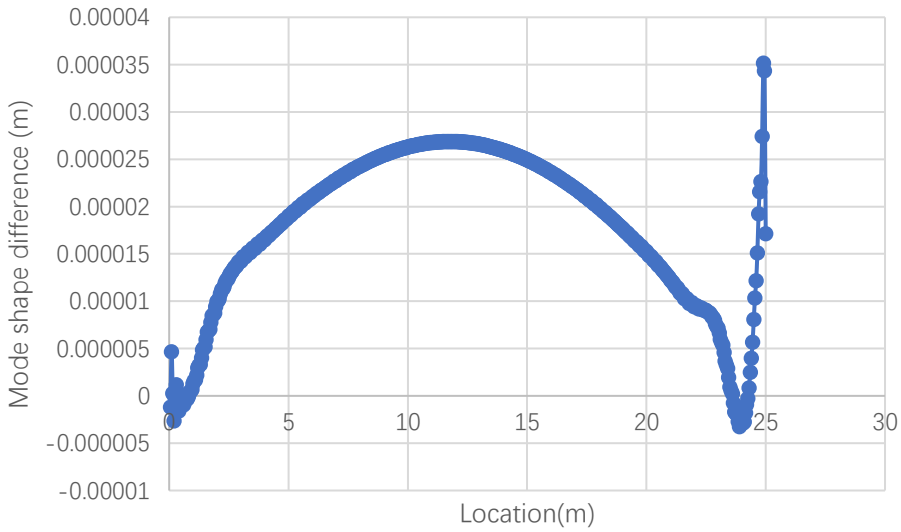

Figure 2.23. Mode shape differences between the 1 m damage bridge and the original bridge

From Figure 2.23, the mode shape difference can not point out the location when damage is at the 1 m location. The same reason that the damage is too close to the support could explain this result.

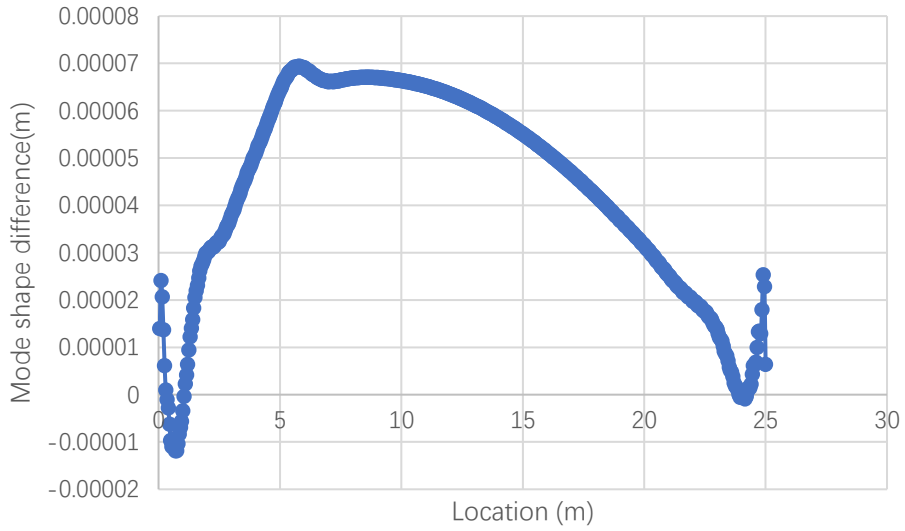

Figure 2.24. Mode shape differences between the 5 m damage bridge and the original bridge

Figure 2.24 shows that there is a sharp upward peak at the 5 m location of the mode shape difference. This can be regarded as a good indicator of the damage.

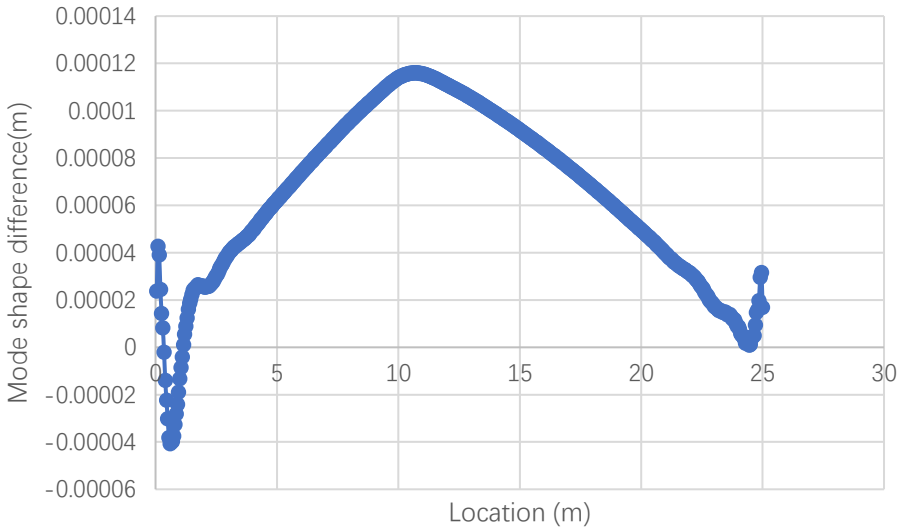

Figure 2.25. Mode shape differences between the 10 m damage bridge and the original bridge

Figure 2.25 shows the same upward peak occurred at the 10 m location, which well corresponds to the actual damage location.

From above results, we can see the mode shape difference method is an alternative method to detect the damage location in 2D BVI simulations. Comparing with the STFT method, mode shape method needs an extra data processing step to show the connection between results and damages.

3. DRIVE-BY DAMAGE IDENTIFICATION THROUGH 3D VIRTUAL SIMULATIONS

3.1. Introduction

In Chapter 2, a 2D bridge-vehicle-interaction (BVI) model has been created to couple the dynamic behaviors of bridges and vehicles. Based on the BVI model created, the STFT method and Mode shape method were used to detect bridge damages and its efficiency has been validated. In this chapter, a 3D bridge-vehicle-interaction model will be generated similar to Chapter 2. The same methods will be also applied to the simulation results to identify damages.

3.2. 3D Vehicle Model Build-up

Following previous study (Oliva, et al., 2013), a 3D vehicle model based on a real truck is created. The model uses the same properties as these of the literature, which includes mass, spring stiffness, damping, and body rotary inertias. The needed vehicle parameters are shown in Figure 3.1. Its specific parameters are given in Table 3.1.

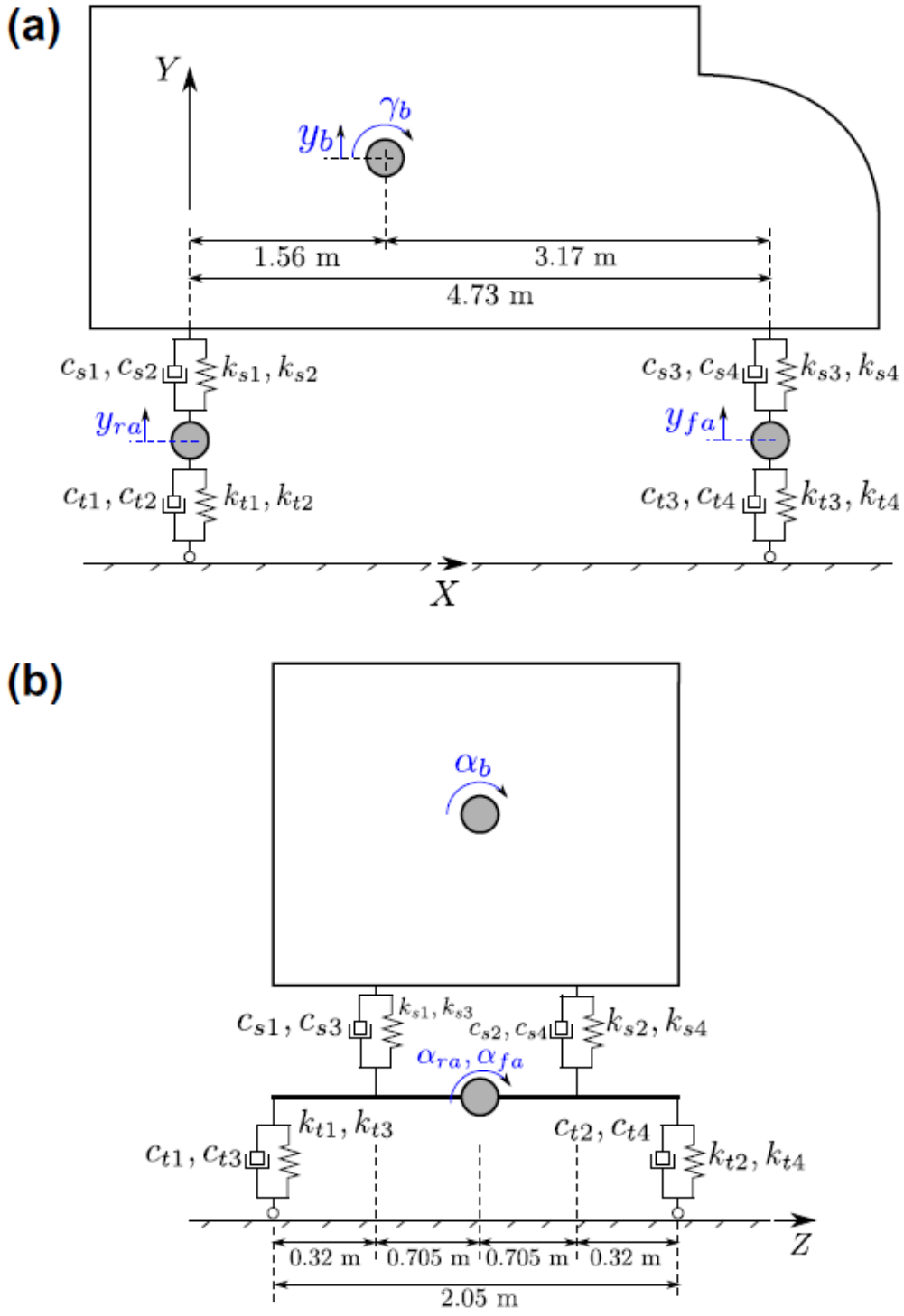

Figure 3.1.Truck model: (a) side view, (b) rear view

Table 3.1. The mechanical parameters of the vehicle

Element	Notation	Value
Stiffness(N/m)		
Rear wheels	K_{t1}, k_{t2}	1.57e6
Front wheels	K_{t3}, k_{t4}	7.85e5
Rear suspensions	$K_{s1,}$ k_{s2}	3.73e5
Front suspension	$K_{s3,}$ k_{s4}	1.16e5
Dampings (N s/m)		
Rear wheels	C_{t1}, C_{t2}	200
Front wheels	C_{t3}, C_{t4}	100
Rear suspensions	$C_{s1,}$ C_{s2}	35000
Front suspension	$C_{s3,}$ C_{s4}	25000
Masses (Kg)		
Rear axle	m_{ra}	1000
Front axle	m_{fa}	600
Body	m_b	17000
Rotatory inertias (kg m^2)		
Rear axle (roll)	$I_{\alpha,ra}$	600
Front axle (roll)	$I_{\alpha,fa}$	550
Body (roll)	$I_{\alpha,b}$	13000
Body (pitch)	$I_{\gamma,b}$	90000

Using these data, the truck model has been created in ABAQUS. All truck bodies are assumed rigid, since the vibration caused by external forces is concerned and the deformation of truck body itself is small and could be neglected. Rigid body needs to have a reference point, which would be set as the geometry center of each part.

For the mass, considering the rotatory inertias, the body part could attach the mass on the reference point with rotatory inertias. However, the axle parts could not simply attach the mass and rotate on the reference point, since this will make the axle to only have vertical displacement without rotation. In solving this issue, the axle mass is divided into 4-point masses, and the locations can be calculated to meet the rotatory inertias. Through these implementations, the

frequency analysis results of the ABAQUS model are quite the same with the literature results. The comparison of the literature results and the current results is shown in Figure 3.2.

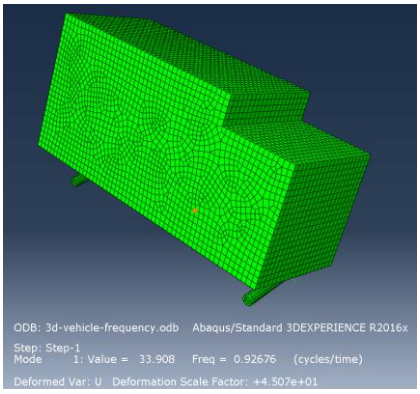

(a) Mode 1 $\longrightarrow f_1 = 0.927$ Hz

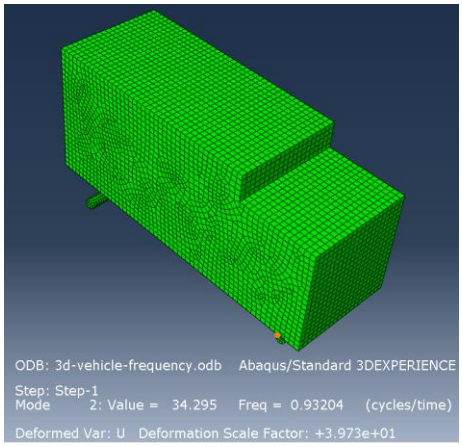

(b) Mode 2 $\longrightarrow f_2 = 0.932$ Hz

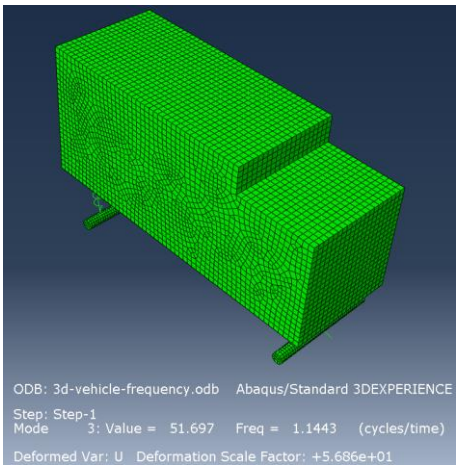

(c) Mode 3 $\longrightarrow f_3 = 1.144$ Hz

Figure 3.2. Comparison of the model vehicle frequencies with the literature results. (a) Model 1, (b) Model 2, (c) Model 3, (d) Model 4, (e) Model 5, (f) Model 6, (g) Model 7

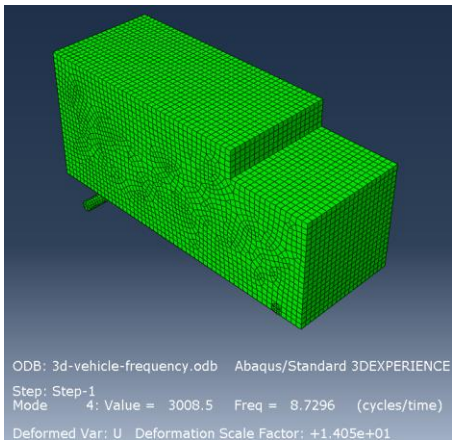

(d) Mode 4 $\longrightarrow f_4 = 8.730$ Hz

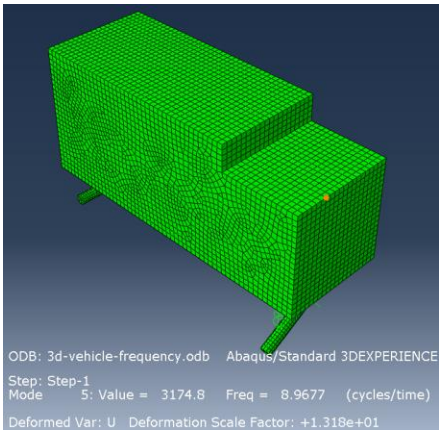

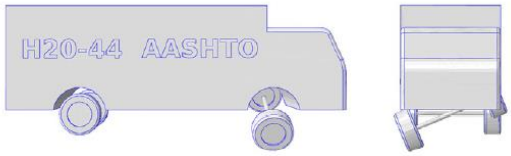

(e) Mode 5 $\longrightarrow f_5 = 9.016$ Hz

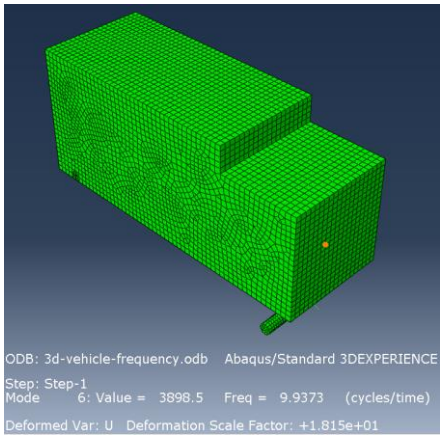

(f) Mode 6 $\longrightarrow f_6 = 9.937$ Hz

Figure 3.2. Comparison of the model vehicle frequencies with the literature results (continued). (a) Model 1, (b) Model 2, (c) Model 3, (d) Model 4, (e) Model 5, (f) Model 6, (g) Model 7

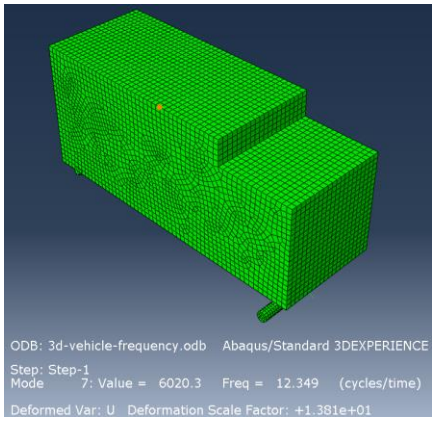

(g) Mode 7 $\longrightarrow f_7 = 12.450$ Hz

Figure 3.2. Comparison of the model vehicle frequencies with the literature results (continued). (a) Model 1, (b) Model 2, (c) Model 3, (d) Model 4, (e) Model 5, (f) Model 6, (g) Model 7

3.3. 3D Multiple Span Bridge Model

A 3D multiple span bridge is created based on a previous research (Olivia, et al, 2010) and used to test the drive-by inspection hypothesis in this thesis.

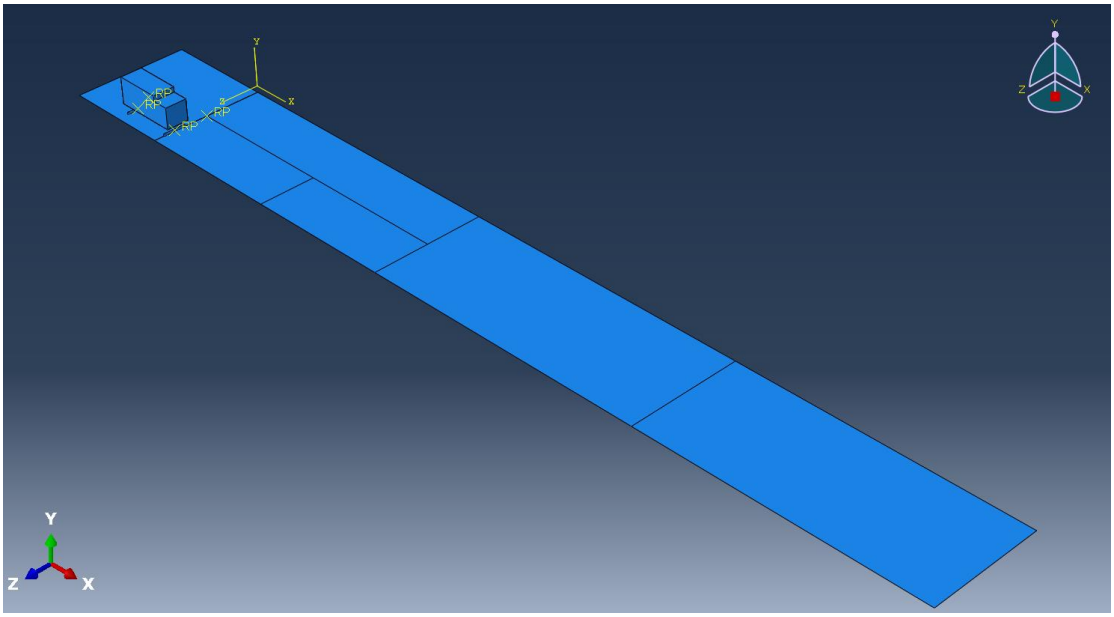

Figure 3.3. 3D multi-span bridge model

The bridge is 79.2 m long in total, with three 26.4 m spans. The width is 10.7 m, and the depth is 0.95 m. Young's modulus is 14.54e10 N/m^2, Poisson's ratio is 0.3, and the density of the

bridge material is 2375 kg/m^3. The vehicle crosses the bridge with its right tires at a distance of 1 m from the bridge right span edge.

The left boundary of the bridge is fixed, while the two intermediate supports and the right boundary only have the lateral movement allowed. A similar mesh size study is conducted and shown in Figure 3.4. The results suggest that mesh size under 0.1 is adequate and convergent in capturing bridge displacement. In the later simulations of this model, 0.1 m is chosen as the mesh size.

The first mid span vertical displacement results are recorded and compared with the literature results in Figure 3.5, when the truck passes the bridge with a speed of 32.0 m/s.

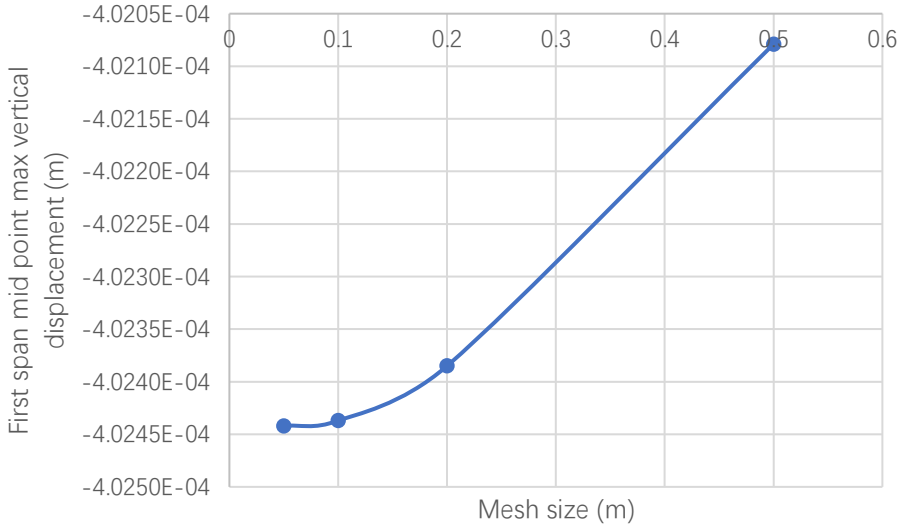

Figure 3.4. Mesh sensitivity plot for the 3-span bridge

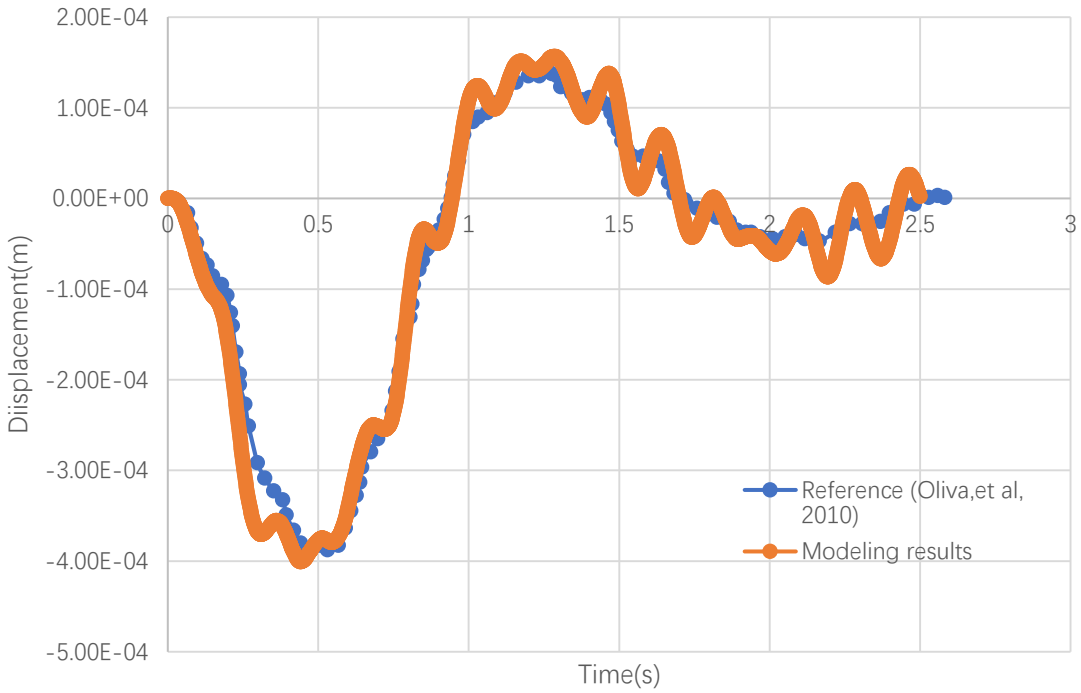

Figure 3.5. The mid-span displacement time history of the first span when the truck passes at 32.5 m/s

From Figure 3.5, we could see the numerical model captures the bridge and vehicle interaction quite accurately.

3.4. Bridge Frequencies Detection through Vehicle Responses

When vehicle speed decreases to 1 m/s, same as part 2, the FFT results of the vehicle front body accelerations can be used to identify frequencies of the truck and the bridge (Figure 3.6).

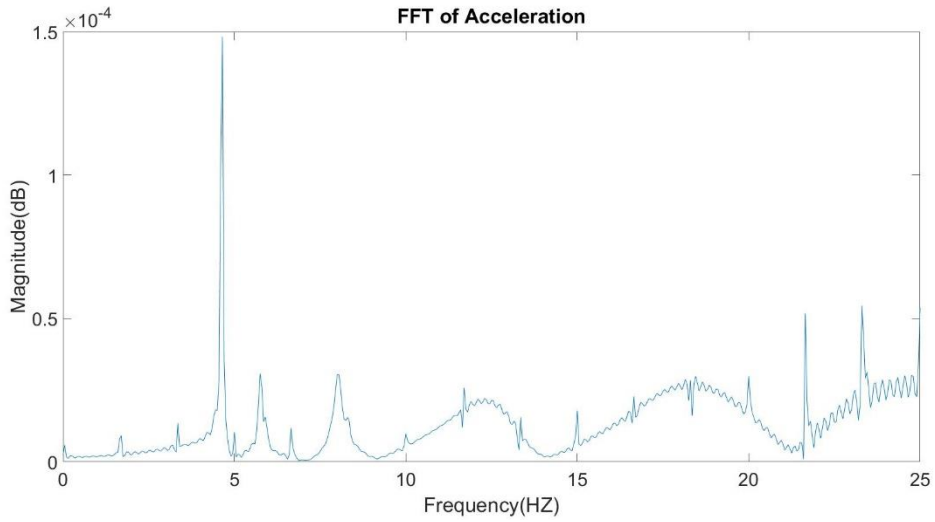

Figure 3.6. The identified frequencies using the front tire acceleration time history

Using the vehicle vertical acceleration data collected from the front tire, bridge frequency values can be identified, which are shown in Figure 3.6 and Table 3.2.

Table 3.2. The identified bridge frequencies through the front tire acceleration time history

	Reference Bridge Frequencies (Hz)							
Property	4.83	6.21	9.13	16.23	17.24	18.57	18.91	20.94
FFT Results	4.65	6.65	10	16.65		18.45		20

Table 3.2 shows that most bridge frequencies can be identified through the FFT results of the vehicle's vertical acceleration.

3.5. STFT of Vehicle Responses and Its Relationship with Damage

In order to demonstrate the effectiveness of STFT in 3D bridge damage detections, a simply supported short bridge will be used to filter out the effect of internal supports. The bridge has the properties shown in Table 3.3.

Table 3.3. Properties of the simulated short bridge

Length	15 m	Young's modulus	3E10 N/m^2
Width	10 m	Poisson's modulus	0.2
Thickness	1 m	Density	2500 Kg/m^3
Damping	2%		

A similar sensitivity study is conducted and shown in Figure 3.7. The plot shows that the middle span displacement does not change much when mesh size is blow 0.1 m. Based on this, mesh size for the bridge model is chosen as 0.1 m.

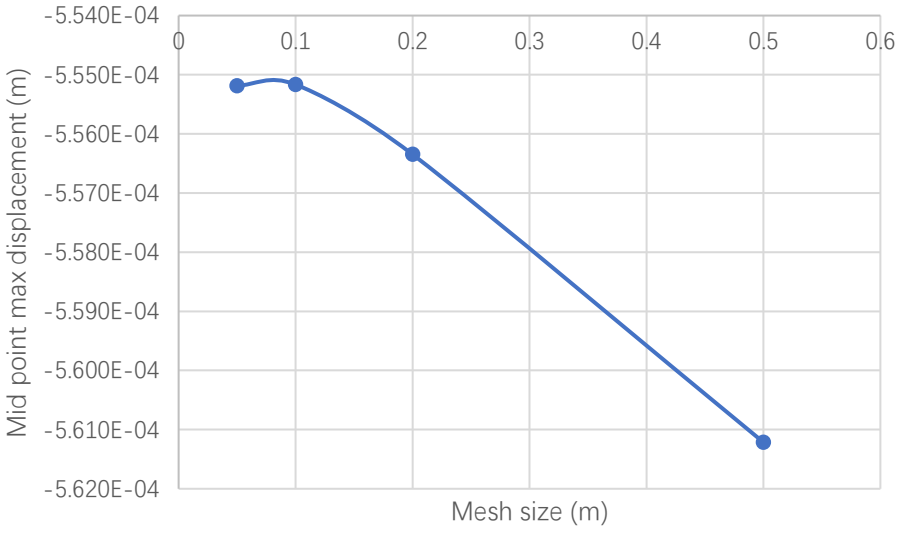

Figure 3.7. Mesh sensitivity plot

When the tire moves on the damaged bridge, the vibration of the vehicle will be changed and this would cause the STFT results show multiple high energy frequencies between 20 Hz to 50 Hz (Figure 3.8). The similar changes will occur when the front tire drives out of the bridge or the rear tire drives in the bridge. The acceleration data is collected from the rear tire because the frequency changes caused by the front tire driving out the bridge are smaller than these caused by the rear tire on the damaged bridge. The underlying reason could be explained as the front tire is

acting as an actuator while the rear tire is acting as a sensor to pick up the signal excited and accumulated through time.

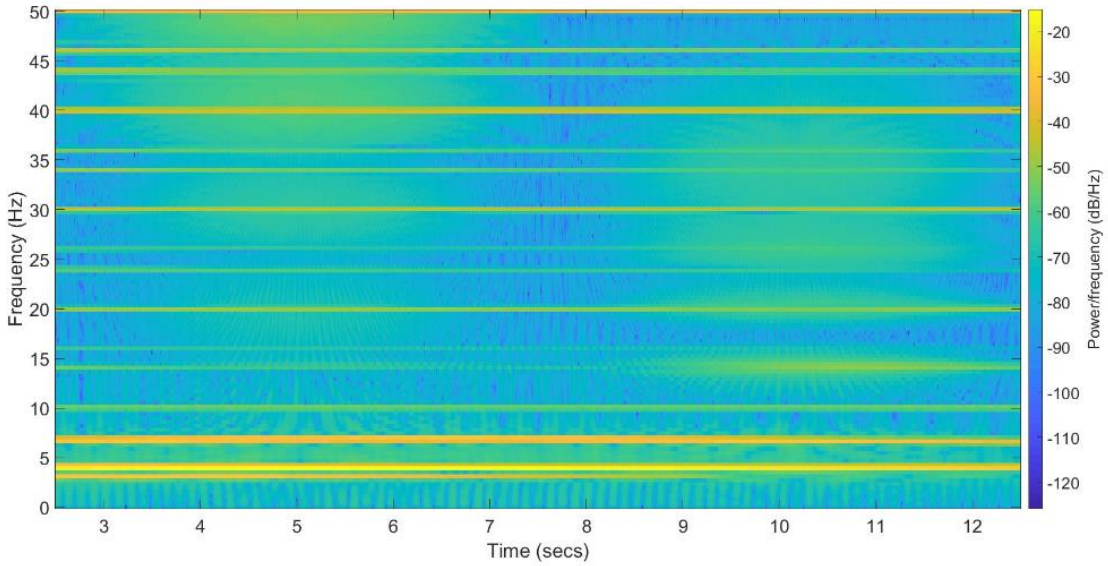

Figure 3.8. STFT result of the bridge deck with a 10cm damage at 5m through the drive-by front tire acceleration time history

To identify the damage, 10% energy difference of the frequency range between 47 Hz to 50 Hz is set as the threshold for damage identification.

To simulate different damage locations, a 10 cm segment with 80% original Young's modules is set at 5.0 m, 7.5 m and 10 m of the bridge. The predicted damage locations are listed in Table 3.4 for the purpose of comparison.

Table 3.4. Comparison of the predicted and real damage locations

Cases	Real mid location(m)	Identified results			
		Start location (m)	End location (m)	Mid location (m)	Ave energy (dB)
0.1 m damage at 5 m location	5.05	4.81	5.3	5.05	-88.06
0.1 m damage at 7.5 m location	7.55	7.21	7.85	7.53	-87.734
0.1 m damage at 10 m location	10.05	9.05	10.95	10.0	-106.867

From Table 3.4, we could see the damage location has been identified successfully through the vehicle's vertical acceleration history.

To reflect effect of the damage severities, a 10 cm segment with 20%, 40% and 60% loss of original Young's modules is set at 7.5 m. The change of frequency energy can be plotted with the modules loss as shown in Figure 3.9.

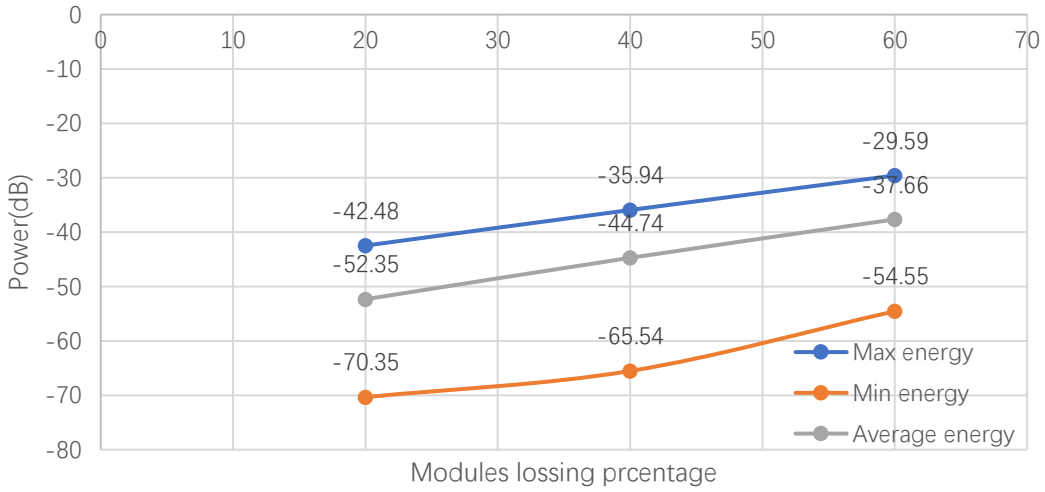

Figure 3.9. STFT energy results for different damage levels

From Figure 3.9, the energy changes for each spectrum frequency has a linear relationship with the damage level of the bridge deck.

3.6. Mode Shape Analysis Results

Using the mode shape method mentioned in chapter 2, the mode shapes of the 3D bridge mode can also be extracted. However, because the data is only collected from one point of vehicle axle, the extracted mode shapes are one cross-section of the whole 3D mode shapes.

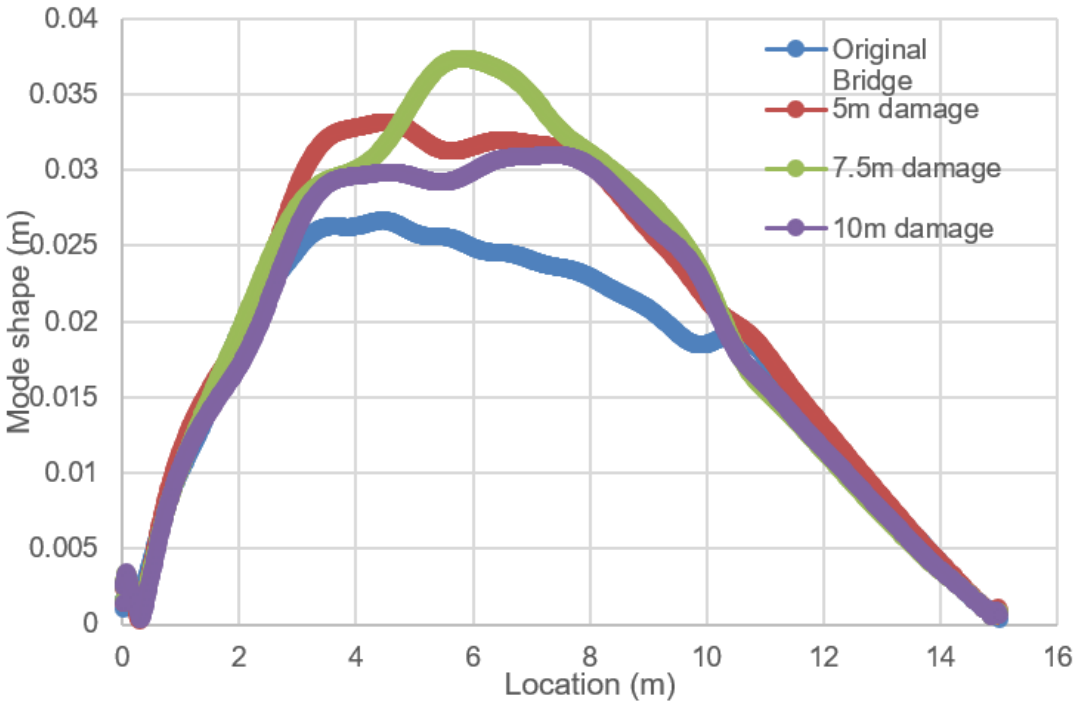

Figure 3.10. First mode shape of 4 different bridges

The mode shape frequency filter is set at 7.0 Hz, which is the same as the first bridge frequency that can be captured by the vehicle. From Figure 3.10, this extracted mode shape is quite similar with the deformed shape of bridge when frequency is 7.0 Hz. There is a downward sharp change at 5m, which accurately indicates the damage location.

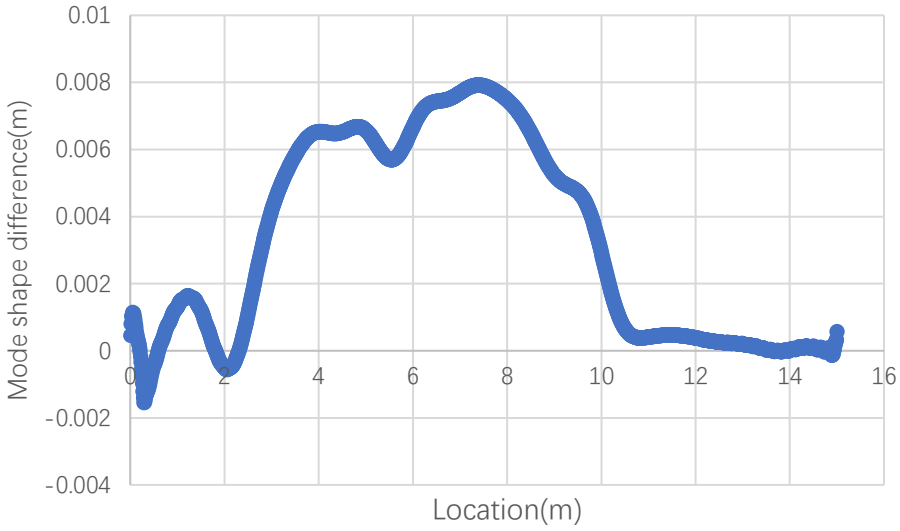

Figure 3.11. Mode shape differences between the 5 m damage bridge and the original bridge

Figure 3.12 shows the mode shape difference between the 7.5 m damage bridge and the original bridge, there is a sharp peak change between the 5 m and 8 m locations on the bridge. Besides this, there are also some small mode changes between 0 m to 2 m locations on the bridge. This may be due to the influence of supports.

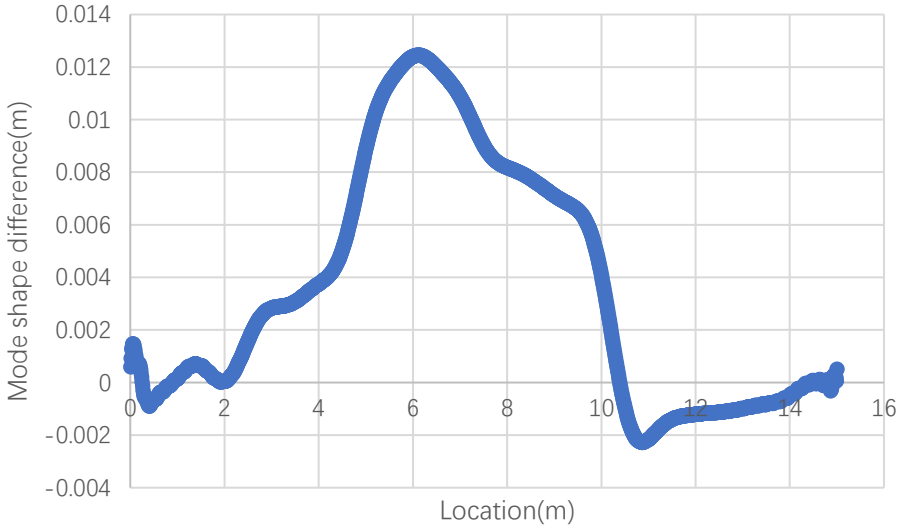

Figure 3.12. Mode shape differences between the 7.5 m damage bridge and the original bridge

A similar change can be found when the damage moves to 10 m (Figure 3.12).

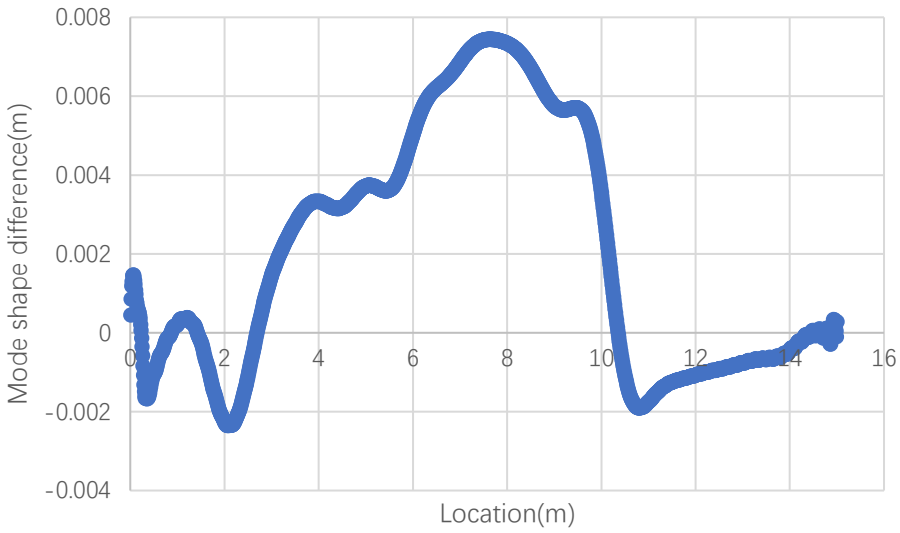

Figure 3.13. Mode shape differences between the 10 m damage bridge and the original bridge

In Figure 3.13, damage caused mode change happens between 6-10 m, however the change gest blurred at the 10 m location because the damage location is close to the place where the vehicle front axle is driving off the bridge.

Considering the results of these three plots, the mode shape difference has the potential to identify the damage location through the vehicle's vertical acceleration history.

4. EFFECT OF ROAD ROUGHNESS ON DRIVE-BY BRIDGE INSPECTION

In this chapter, road roughness will be added into the 3D model to study how it will affect the drive-by detection of damages on bridges.

4.1. Road Roughness Generation

According to the ISO standard 8608, road surface profiles can be represented with a zero-mean normal stationary ergodic random process described by their Power Spectral Density. The PSD can be described by the following function:

$$G(n) = G(n_0)\left(\frac{n}{n_0}\right)^{-2} \tag{5}$$

The $G(n)$ is the power spectral density for the spatial frequency n and $G(n_0)$ is the power spectral density for the reference spatial frequency n_0= 0.1 m^{-1}. The value of $G(n_0)$ represents the road profile class.

Table 4.1. Road roughness classification

Road class	$G(n_0)$ (m^3)
A(very good)	1.600E-05
B(good)	6.400E-05
C(medium)	2.560E-04
D(poor)	1.024E-03
E(very poor)	4.096E-03

Road profiles could be generated as the sum of a series of harmonics:

$$y_1(x) = \sum_i^N \sqrt{2G(n_i)\Delta n}cos\ (2\pi n_i x + \emptyset_i) \tag{6}$$

In this study, Class B road profile is chosen to be simulated in the 3D BVI model. The profile is generated through Matlab, then written into the 3D bridge model through the ABAQUS input file. The steps used in road roughness generation are listed as following:

1. Establish the original bridge in ABAQUS, and generate an input file of the model;
2. Generate a 2D roughness profile with 151 x 101 node points. The profile is generated line

by line in the vehicle moving direction using Equation (6). Each line is different from each other, but the trend of each line is the same.

3. Reshape the roughness amplitude matrix into one column, and replace the node coordinate inputs in the ABAQUS input file with the generated roughness node coordinates.

In Figure 4.1, the plot shows a generated road roughness from Matlab, for a class B road roughness. Figure 4.2 shows the PSD plot of the generated roughness which displays a linear fitted relationship between spatial frequencies and displacement PSDs with a fitting coefficient close to -2. The -2 slope obtained verifies Equation (5) and the road profile generated.

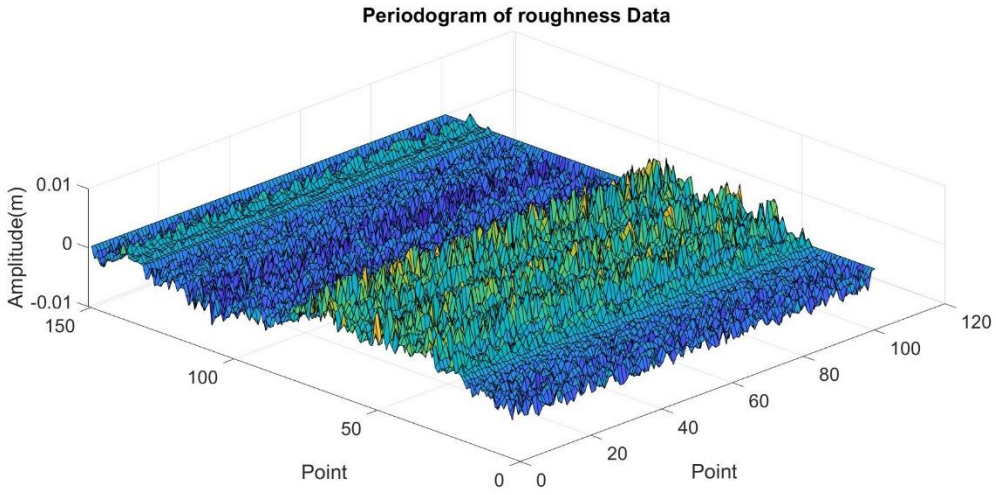

Figure 4.1. Class B road roughness generated

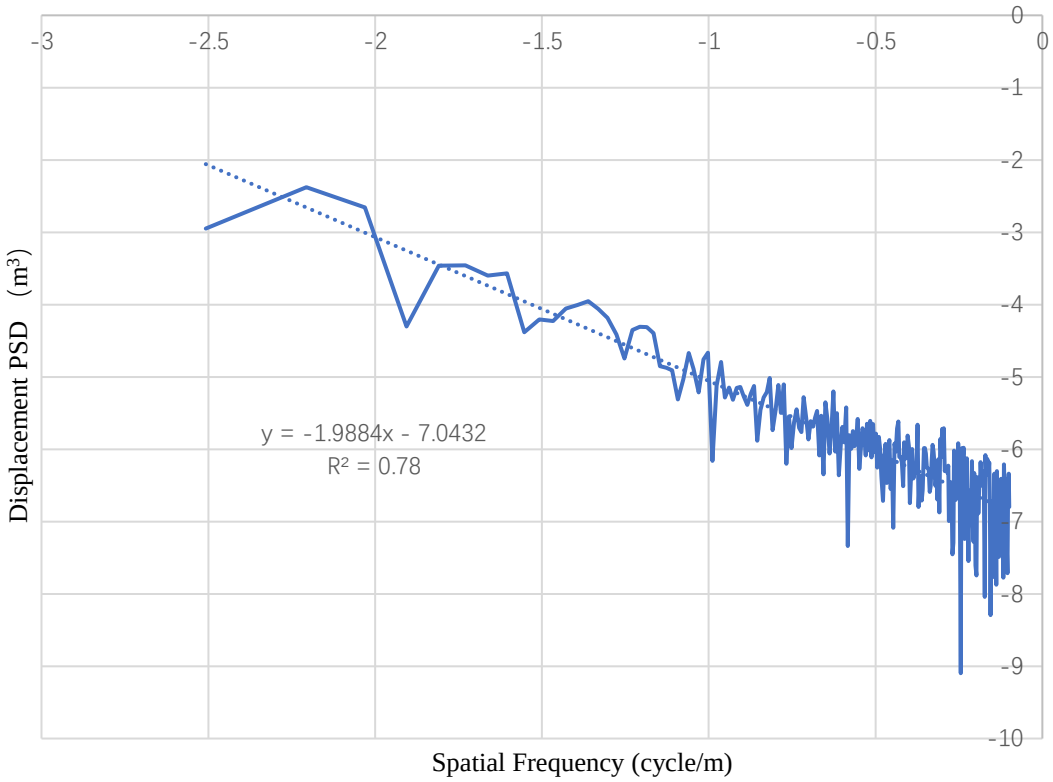

Figure 4.2. Displacement PSDs versus spatial frequencies

4.2. Effect of Roughness on Initial Conditions of BVI Interaction Simulations

Initial vehicle status can affect the detection of bridge properties, which has been verified by Y. B. Yang (2005). In order to find how the road roughness affects vehicle status, a series of model simulations are conducted.

A 30 by 10 m ground is generated in Abaqus. It has the same property as the short bridge. The vehicle will drive through the ground in 10 m/s, 20 m/s, 25 m/s and 30 m/s with 4 different offset distances with the bridge entrance. The displacement, velocity, and acceleration amplitude of the vehicle when entering the bridge will be compared. Four plots of the right front axle acceleration history of the vehicle is shown in Figure 4.3 to Figure 4.6.

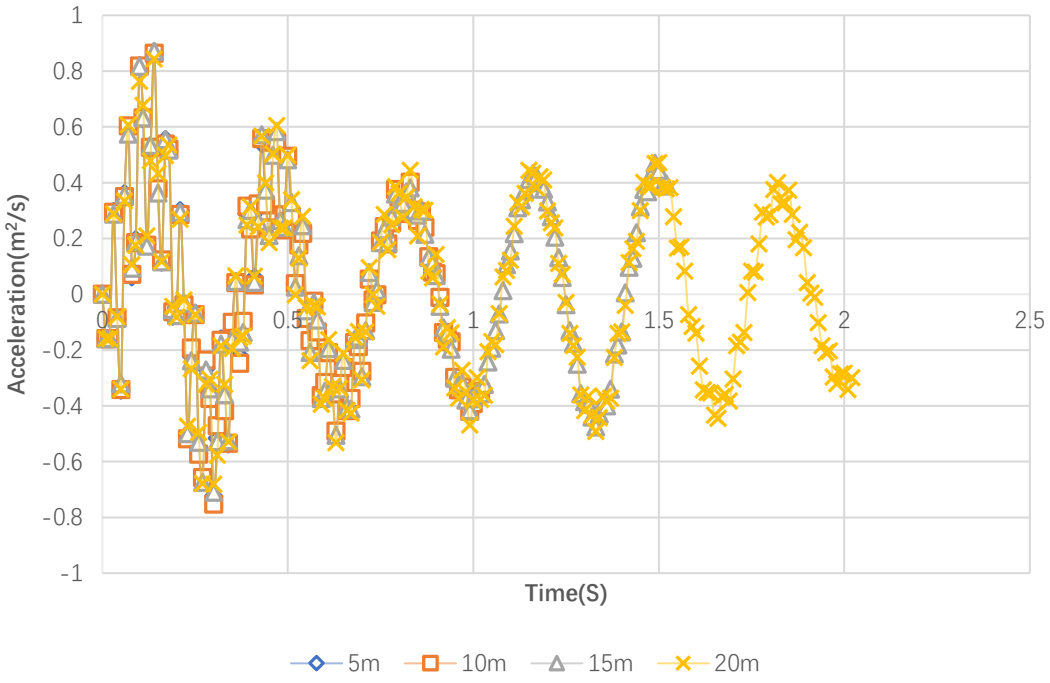

Figure 4.3. Right front axle acceleration history when approaching the bridge at 10 m/s

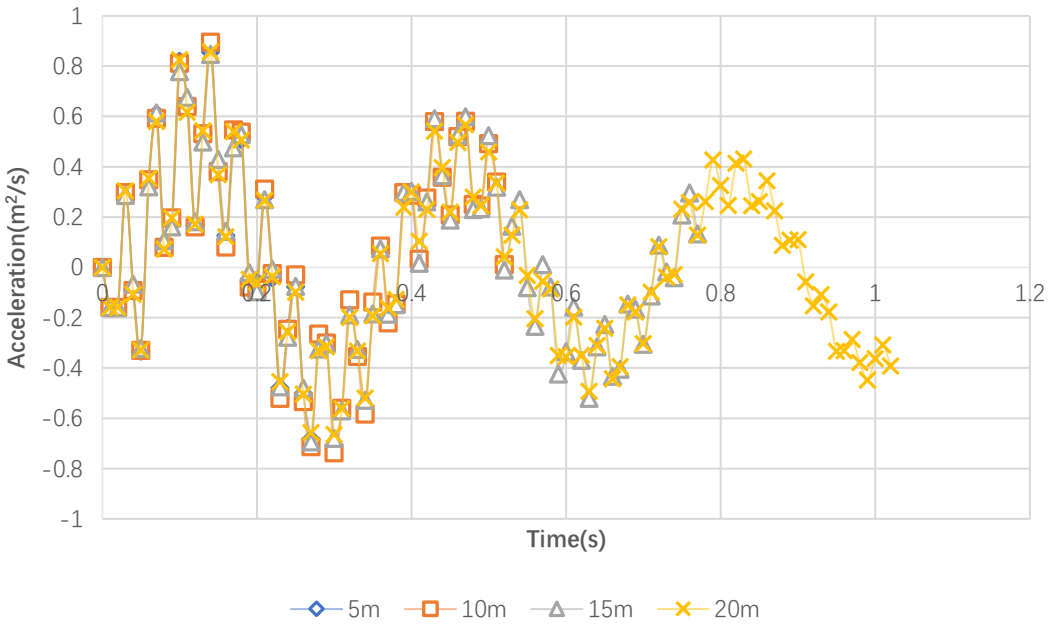

Figure 4.4. Right front axle acceleration history when approaching the bridge at 20 m/s

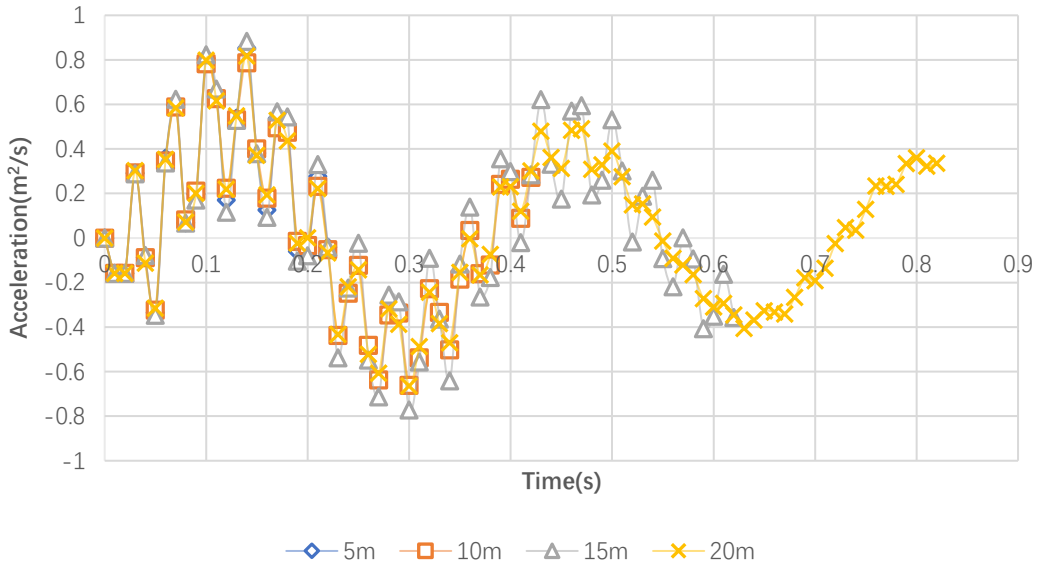

Figure 4.5. Right front axle acceleration history when approaching the bridge through 25 m/s

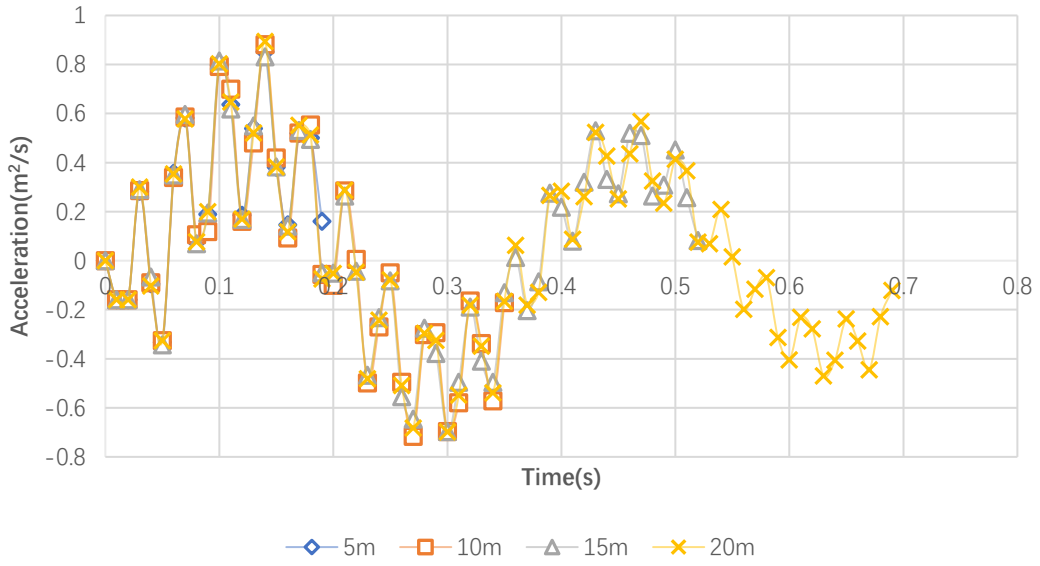

Figure 4.6. Right front axle acceleration history when approaching the bridge through 30 m/s

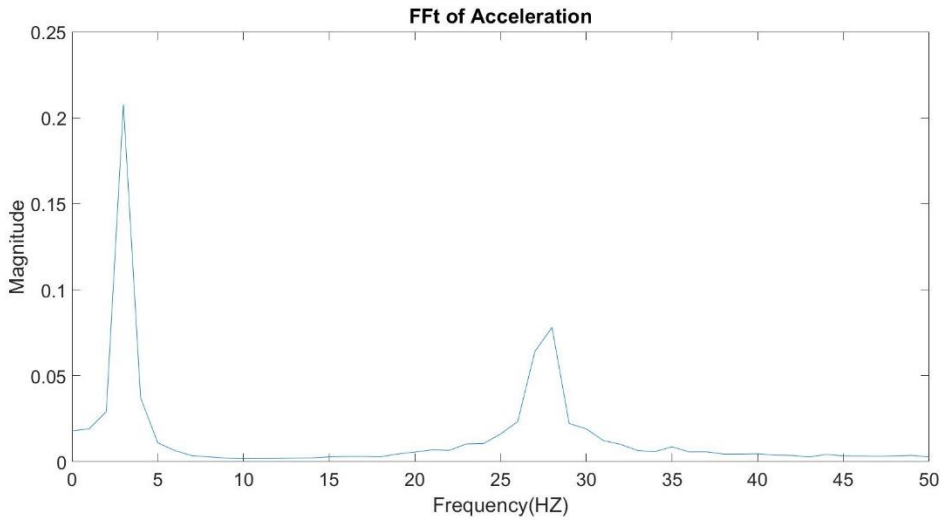

Figure 4.7. FFT Results of the vehicle acceleration responses when driving from a 20 m offset distance with a speed of 10 m/s

FFT Results of the vehicle acceleration responses when driving from a 20 m offset distance with a speed of 10 m/s is shown in Figure 4.7, which shows that there are two acceleration vibration frequencies. One frequency is at 3 Hz, while the other one is at 28 Hz.

Table 4.2. Acceleration amplitude for the 3 Hz component in the vehicle's vibration

		Driving Distance			
		5 m	10 m	15 m	20 m
Driving Speed	10 m/s	0.393	0.384	0.423	0.312
	20 m/s	0.491	0.412	0.373	0.377
	25 m/s	0.511	0.498	0.384	0.341
	30 m/s	0.518	0.508	0.386	0.352

Table 4.3. Acceleration amplitude for the 28 Hz component in the vehicle's vibration

		Driving distance			
		5 m	10 m	15 m	20 m
Driving speed	10 m/s	0.14	0.036	0.003	0.021
	20 m/s	0.202	0.124	0.103	0.07
	25 m/s	0.285	0.211	0.121	0.019
	30 m/s	0.334	0.266	0.123	0.116

From the two amplitude results, the vibration of the vehicle keeps decreasing with longer driving distance. This decreasing is caused by damping of the vehicle. And with the driving speed increasing, the end amplitude becomes larger. This is because the damping of vehicle does not have enough time to release the energy. However, to simulate a BVI model accurately, it is important to set adequate driving distance from the entrance of the bridge. Otherwise, additional frequencies will be included in the model and affect the simulation accuracy. In this chapter, 10 m offset distance is needed for speed less than 20 m/s, 15 m offset distance is needed for speed between 20-25 m/s, while more than 20 m offset distance is needed for speed at 30 m/s and above.

4.3. Road Roughness and Bridge Frequency

Using the same method, the Class B road profile can be added to the short bridge surface. The vehicle is driven through the bridge with a speed of 1 m/s. As the rear axle goes through the whole length of the bridge, the acceleration data is collected from the right rear axle.

After FFT process of the collected acceleration data from the right rear axle, the results can be showed in Figure 4.8

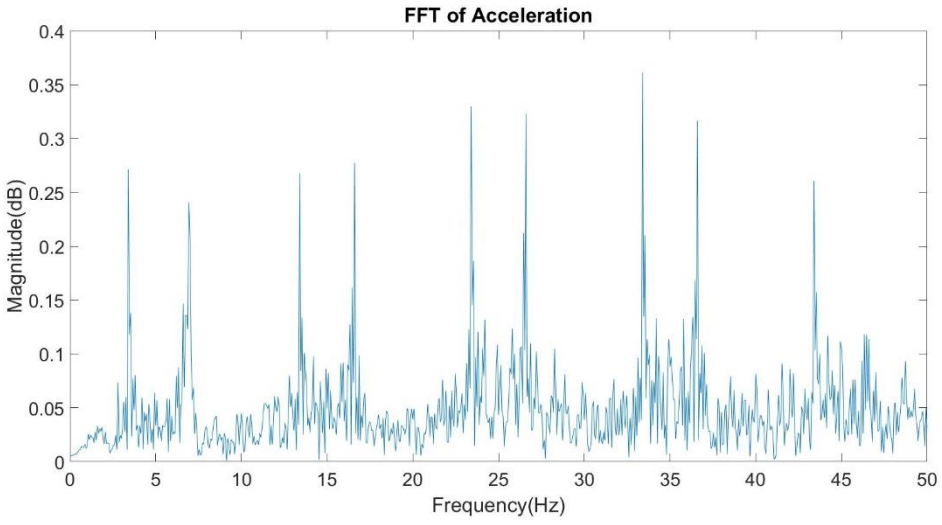

Figure 4.8. FFT results of acceleration history of the BVI model with road roughness

The comparison of identified results and reference bridge frequencies are listed in Table 4.4.

Table 4.4. Identified bridge frequencies and the theoretical bridge frequencies (Hz)

	Bridge Frequencies								
Theoretical bridge frequency		7		15.4		28		38.6	
Identified frequency	3.4	6.94	13.4	16.6	23.4	26.6	33.4	36.6	43.4

From Table 4.4, we could see the drive-by inspection could identify most of the bridge frequencies.

4.4. Effect of Road Roughness on STFT Damage Detection

After the road roughness is superimposed onto the bridge deck, a test of damage detection is conducted through the 3D BVI model with embedded damages. Its STFT and mode shape analysis results are shown in Figure 4.9-4.13.

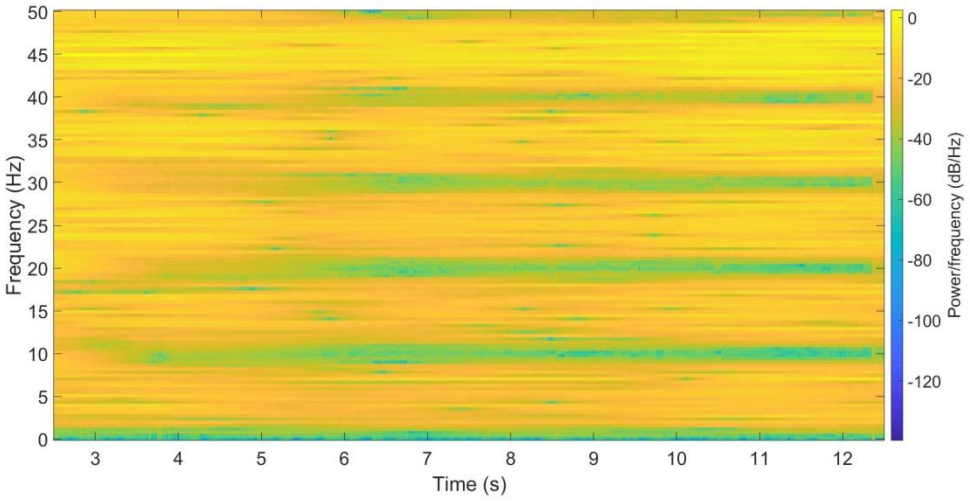

Figure 4.9. STFT results of no undamaged bridge with roughness

The STFT results show that there is much roughness noise signal. To reduce the effect of roughness, the vibration differences between healthy bridge and damaged bridge are used to

process the STFT analysis results. A 0.1 m damage with 40%, 60% and 80% of the original Young's modulus is set at the mid-span of the bridge.

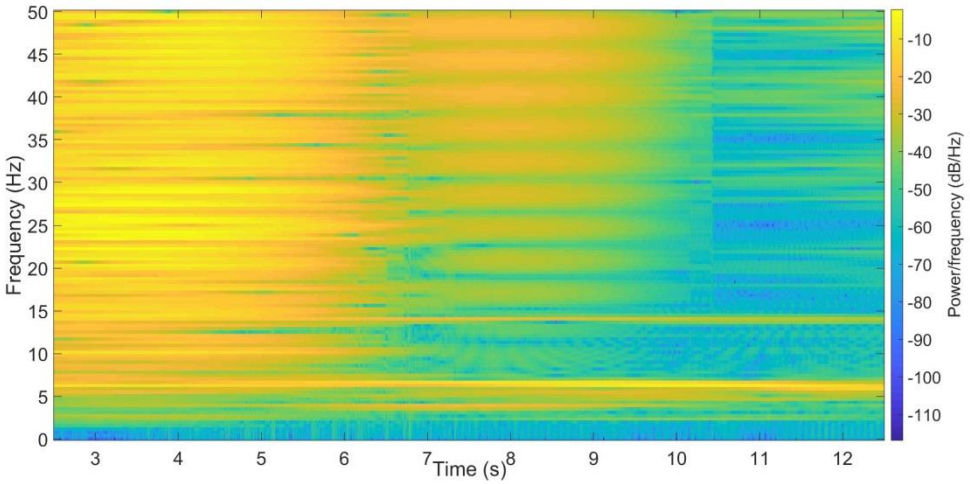

Figure 4.10. STFT results of acceleration difference between the 40% damage case and the healthy bridge

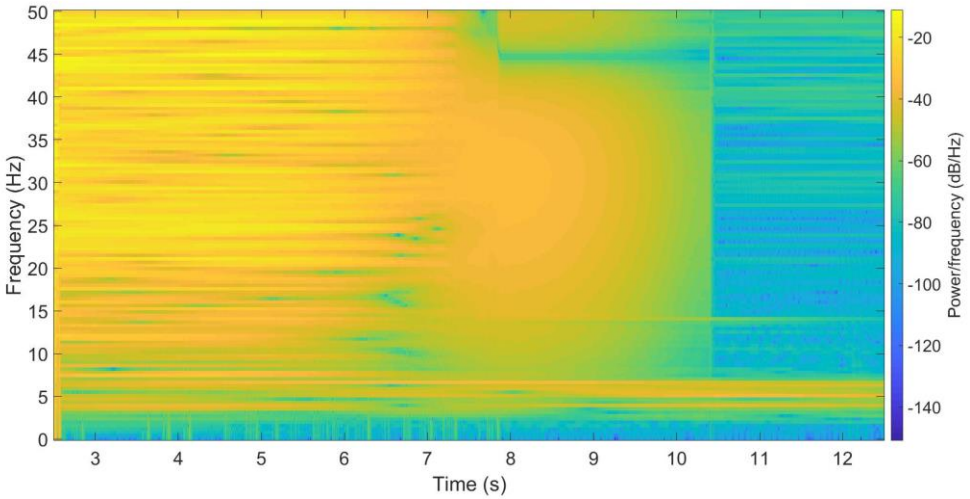

Figure 4.11. STFT results of acceleration difference between the 60% damage case and the healthy bridge

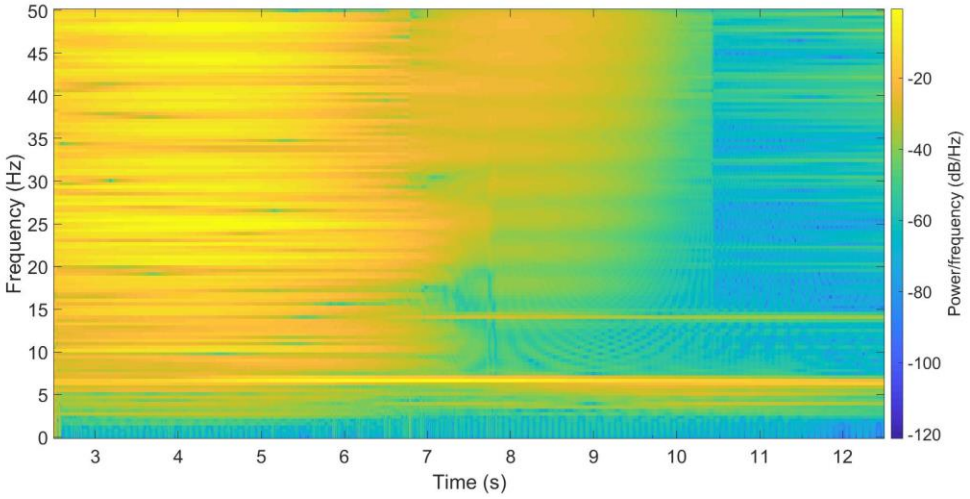

Figure 4.12. STFT results of acceleration difference between the 80% damage case and the healthy bridge

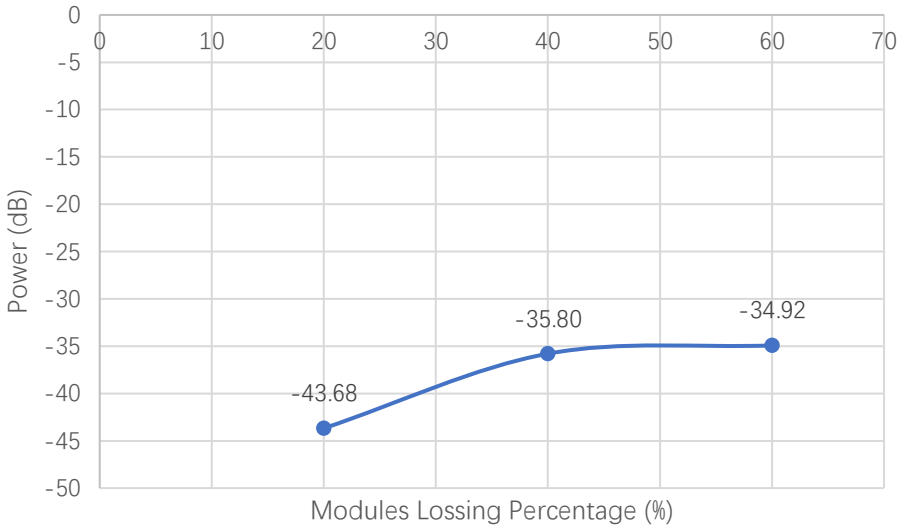

Figure 4.13. Average SPD energy over the damaged area (7.5 m to 7.6 m)

In these 3 plots, the differences can not reduce all roughness effect. However, the frequencies between 20 Hz to 50 Hz have obvious changes at 7.5m according to different damage levels. The STFT method still has the potential to identify different damages of bridges with consideration of roughness effect.

4.5. Road Roughness and Mode Shape Damage Detection

In this part, 2 damage models are analyzed. A 0.1 m damage is set at the 5 m and 10 m location over the bridge, respectively. Acceleration differences between the damaged and healthy bridge are used to extract bridge frequencies and identify damages.

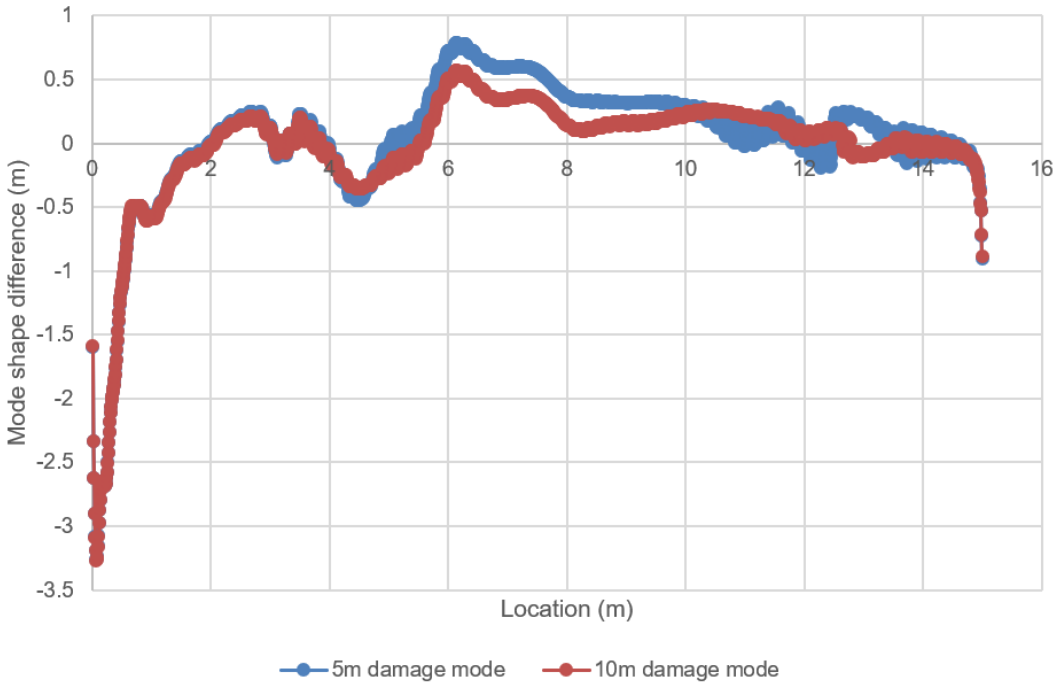

Figure 4.14. Mode shape difference of vehicle acceleration for two damaged bridges

In Figure 4.14, the mode shape differences show the peak value changing at 6 m and 10 m. These changes directly connect with the damage area, which indicate that the mode shape method has its potential on detecting damage areas in bridges with consideration of roughness effect.

5. SUMMARY AND CONCLUSIONS

5.1. Introduction

Summary of the research and conclusions derived from this research are presented in this chapter. In order to study the damage detection capacity of drive-by vehicles, both 2D and 3D finite element models were built in this research. Using the STFT method and mode shape method, damage can be identified through collected data from drive-by vehicles. The limitations of the current study and the recommendations for future work are also discussed.

5.2. Summary

In this research, a 2D Bridge-Vehicle-Interaction finite element model is established through ABAQUS first. With simulated damages, the relationship of different damages and FFT results of drive-by vehicle vertical accelerations is analyzed. STFT method and mode shape method are then used to capture bridge damage locations and severities. The possibility and accuracy of identifing damages through drive-by vehicles are analyzed through comparison of the collected vehicle signals with different damaged bridges,. Further, a 3D bridge-vehicle-interaction finite element model is established and verified. The frequencies identified on multi-span bridges through drive-by vehicles are checked with respect to literature results. The STFT method and mode shape method are then used to analyze the difference between damaged and undamaged 3D bridges and show their capability in identifying bridge damages.

5.3. Conclusions

Based on a series of 2D and 3D virtual BVI simulations conducted in this thesis, the following conclusions are derived:

- FFT of vehicle accelerations through drive-by inspection can capture bridge frequencies accurately. In the 2D BVI model, the captured frequencies can reflect the

damage with a decrease in their magnitudes. In the 3D BVI model, the FFT method can capture most frequencies of multiple span bridges with high accuracy, even with damages included.

- STFT method works well in identifying damages through drive-by vehicle responses in the BVI models. Energy change in STFT results of drive-by vehicle responses can identify the damage location and the damage level in high accuracy.
- Vibration caused by roughness will be introduced during driving and affects the initial entering conditions of vehicles in the BVI models. The possible effect of roughness on drive-by damage identification of bridges with rough surfaces has been summarized. Moreover, the offset distances of vehicle before entering bridge are found to grantee the real and accurate bridge and vehicle responses through BVI simulations, which requires a 10 m offset distance for speed less than 20 m/s, a 15 m offset distance for speed between 20-25 m/s, and more than 20 m offset distance is needed for speed over 30 m/s. .
- Roughness increases the difficulty in identifying bridge damages though drive-by vehicle responses. However, both the STFT and mode shape method still have the capability of detecting damage level and damage location in bridges.

5.4. Future Work

This research work is based on 2D and 3D finite element modeling. Limitation of model mesh and time step increment will affect the accuracy of the modeling results. Moreover, the BVI model needs to be verified in practice. Future lab and field experiments could help to strength and refine the approach.

REFERENCES

Yang, Y.-B., Lin, C.W., & Yau, J.D., Extracting bridge frequencies from the dynamic response of a passing vehicle, Journal of Sound and Vibration 272 (3-5), 2004, 471-493

Yang, Y.-B., & Lin, C.W., Vehicle-bridge interaction dynamics and potential applications, Journal of Sound and Vibration 284 (1-2), 2005, 205-226

Yang, Y.-B. & Lin, C.W., Use of a passing vehicle to scan the fundamental bridge frequencies: An experimental verification, Engineering Structures 27(13), 2005, 1865-1878

Yang, Y.-B. & Chang, K.C., Extracting the bridge frequencies indirectly from a passing vehicle: Parametric study, Engineering Structures 31 (10), 2009, 2448-2459

Yang, Y.-B., Li, Y.C., & Chang, K.C., Constructing the mode shapes of a bridge from a passing vehicle: a theoretical study, Smart Structures and Systems 13 (5),2014,797-819

González, A., Covian, E. & Madera, J., Determination of bridge natural frequencies using a moving vehicle instrumented with accelerometers and GPS, Proceeding of the Ninth International Conference on Computational Structures Technology (CST),2008

González, A., OBrien, E., & McGetrick, P., Detection of Bridge Dynamic Parameters using an Instrumented Vehicle, Proceedings of the Fifth World Conference on Structural Control and Monitoring (5WCSCM),2010

González, A., OBrien, E., & McGetrick, P., Identification of damping in a bridge using a moving instrumented vehicle, Journal of Sound and Vibration 331(18), 2012, 4115-4131

González, A., OBrien, E., & McGetrick, P., Using instrumented vehicles to detect damage in bridges, 15th International Conference on Experimental Mechanics, 2012

Zhang, Y., Wang, L. & Xiang, Z., Damage detection by mode shape squares extracted from a passing vehicle, Journal of Sound and Vibration,331 (2), 2012, 291-307

Sun, Z., Nagayama, T. & Su, D., et al, A damage detection algorithm utilizing dynamic displacement of bridge under moving vehicle, Shock and Vibration,2016

Malekjafarian, A. & OBrien, E.J., Identification of bridge mode shapes using Short Time Frequency Domain Decomposition of the responses measured in a passing vehicle, Engineering Structures. 81, 2014, 386-397

Malekjafarian, A. & OBrien, E.J., A mode shape-based damage detection approach using laser measurement from a vehicle crossing a simply supported bridge, Structural Control and Health Monitoring, 23,2016, 1273-1286

Kong, X., Cai, C. & Kong, B., Numerically extracting bridge modal properties from dynamic responses of moving vehicles, Journal of Engineering Mechanics, 2016, 142 (6)

Kong, X., Cai, C., Deng, L. & Zhang, W., Using Dynamic Responses of Moving Vehicles to Extract Bridge Modal Properties of a Field Bridge. Journal of Bridge Engineering. 2017, 22 (6)

Nguyen, K. V. & Tran, H. T., Multi-cracks detection of a beam-like structure based on the on-vehicle vibration signal and wavelet analysis. Journal of Sound and vibration, 2010, 329 (21),

Hester, D. & González, A., A wavelet-based damage detection algorithm based on bridge acceleration response to a vehicle, Mechanical System and Signal Processing 28,2012, 145-166

McGetrick, P. J., & Kim, C. W. A Parametric Study of a Drive by Bridge Inspection System Based on the Morlet Wavelet, Key Engineering Materials, 2013, 569-570, 262-269.

McGetrick, P. J., and Kim, C.W., The use of an instrumented vehicle in a wavelet based damage detection approach for bridge structure, 2nd Int. Conf. on Smart Monitoring, Assessment and Rehabilitation of Civil Structures (SMAR2013)

Liu, X.W., Xie, J. & Wu, C., et al, Semi-analytical solution of vehicle-bridge interaction on transient jump of wheel, Engineering Structures 30(9), 2008, 2401-2412

Oliva, J., Goicolea, J. M., Antolín, P. & Astiz M. Á., Relevance of a complete road surface description in vehicle-bridge interaction dynamics, Engineering Structures, 56, 2013, 466-476

Oliva, J., Goicolea, J. M., Antolín, P. & Astiz M. Á., Finite element models for dynamic analysis of vehicles and bridges under traffic loads, SIMULIA Customer Conference, 2010